



This is a repository copy of *Search for Higgs boson production in association with a high-energy photon via vector-boson fusion with decay into bottom quark pairs at $\sqrt{s} = 13$ TeV with the ATLAS detector.*

White Rose Research Online URL for this paper:

<https://eprints.whiterose.ac.uk/187729/>

Version: Published Version

Article:

Aaboud, M, Aad, G, Abbott, B et al. (2926 more authors) (2021) Search for Higgs boson production in association with a high-energy photon via vector-boson fusion with decay into bottom quark pairs at $\sqrt{s} = 13$ TeV with the ATLAS detector. *Journal of High Energy Physics*, 2021 (3). 268. ISSN 1126-6708

[https://doi.org/10.1007/JHEP03\(2021\)268](https://doi.org/10.1007/JHEP03(2021)268)

Reuse

This article is distributed under the terms of the Creative Commons Attribution (CC BY) licence. This licence allows you to distribute, remix, tweak, and build upon the work, even commercially, as long as you credit the authors for the original work. More information and the full terms of the licence here:

<https://creativecommons.org/licenses/>

Takedown

If you consider content in White Rose Research Online to be in breach of UK law, please notify us by emailing eprints@whiterose.ac.uk including the URL of the record and the reason for the withdrawal request.



eprints@whiterose.ac.uk
<https://eprints.whiterose.ac.uk/>

RECEIVED: October 27, 2020

REVISED: January 27, 2021

ACCEPTED: February 21, 2021

PUBLISHED: March 29, 2021

Search for Higgs boson production in association with a high-energy photon via vector-boson fusion with decay into bottom quark pairs at $\sqrt{s} = 13$ TeV with the ATLAS detector



The ATLAS collaboration

E-mail: atlas.publications@cern.ch

ABSTRACT: A search is presented for the production of the Standard Model Higgs boson in association with a high-energy photon. With a focus on the vector-boson fusion process and the dominant Higgs boson decay into b -quark pairs, the search benefits from a large reduction of multijet background compared to more inclusive searches. Results are reported from the analysis of 132 fb^{-1} of pp collision data at $\sqrt{s} = 13$ TeV collected with the ATLAS detector at the LHC. The measured Higgs boson signal yield in this final-state signature is 1.3 ± 1.0 times the Standard Model prediction. The observed significance of the Higgs boson signal above the background is 1.3 standard deviations, compared to an expected significance of 1.0 standard deviations.

KEYWORDS: Hadron-Hadron scattering (experiments), Higgs physics

ARXIV EPRINT: [2010.13651](https://arxiv.org/abs/2010.13651)

Contents

1	Introduction	1
2	ATLAS detector	3
3	Data and simulated events	4
4	Object selection	5
5	Event selection	6
6	Multivariate analysis	7
7	Signal and background modelling	9
8	Systematic uncertainties	11
	8.1 Experimental uncertainties	11
	8.2 Theoretical uncertainties	12
9	Fit results for Higgs boson production	12
10	Conclusion	15
	The ATLAS collaboration	20

1 Introduction

Following the discovery of a new particle with a mass of approximately 125 GeV by the ATLAS and CMS Collaborations at the Large Hadron Collider (LHC) [1, 2], there has been an extensive effort to measure its properties and compare them with theoretical predictions for the Standard Model (SM) Higgs boson.

Among the Higgs boson production modes still to be explored, the $H\gamma$ mode has received attention for its interesting phenomenology [3, 4], in which the addition of the high-energy photon reorders the usual hierarchy of Higgs boson production cross sections. Experimental measurements are needed to study the SM predictions and to probe for signs of new physics beyond the SM that affect this production mode, which also has potential as a clean signature for unexpected or invisible Higgs boson decays.

The exclusive final state $H\gamma$ is forbidden in gluon-gluon fusion (ggF) by Furry's theorem [5], but the $H\gamma$ system may be produced in recoil against a jet. Contributions from associated WH and ZH production are similar in size to the higher-order contributions from ggF. In vector-boson fusion (VBF), the photon may be radiated either from a charged weak

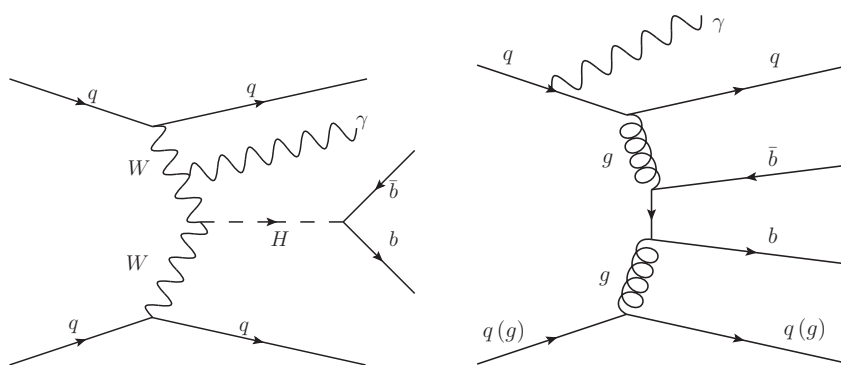


Figure 1. Representative leading-order Feynman diagrams for Higgs boson production via vector-boson fusion in association with a photon (left) and the dominant non-resonant $b\bar{b}\gamma jj$ background (right).

boson or from a scattering quark that showers into a jet (j). VBF is the dominant production mode for $H\gamma$, as its cross section is twice as large as that of all other modes combined.

To select the VBF production mode in particular, a search has been developed in the $H\gamma jj$ final state, with an additional phase-space cut on the jet-jet invariant mass. To maximize the experimental sensitivity to this final state, the search focuses on the dominant $H \rightarrow b\bar{b}$ decay. A previous VBF $H(\rightarrow b\bar{b})\gamma$ search by the ATLAS Collaboration with 31 fb^{-1} of 13 TeV data reported a signal strength measurement, defined as the production rate relative to the SM cross section, of $\mu_{\text{VBF}} = 2.5 \pm 1.9$ and an observed (expected) Higgs boson signal significance of 1.4σ (0.6σ) [6]. A complementary VBF $H(\rightarrow b\bar{b})$ search by the ATLAS Collaboration in an all-hadronic signature, without the associated photon, reported an observed (expected) Higgs boson signal significance of 1.4σ (0.4σ) in the same dataset [6].

In the time since that search was reported, extensive studies of Higgs production without an associated photon by the ATLAS and CMS Collaborations have now accumulated strong evidence for the VBF production mode and for the $H \rightarrow b\bar{b}$ decay. The ATLAS Collaboration has combined several measurements made with up to 79.8 fb^{-1} of 13 TeV data to yield $\mu_{\text{VBF}} = 1.21 \pm 0.23$, compatible with the combined CMS measurement of $\mu_{\text{VBF}} = 0.73 \pm 0.28$ made with up to 35.9 fb^{-1} [7, 8]. Both the ATLAS and CMS Collaborations have observed the $H \rightarrow b\bar{b}$ decay mode, with significances of 6.7σ and 5.6σ respectively, in decay signatures dominated by contributions from WH and ZH production [9, 10].

Nevertheless, there are several interesting effects that motivate testing the SM predictions with a measurement of $H\gamma jj$ production. First, a unique feature of this production mode is that contributions from Z boson fusion are suppressed, due to destructive interference between matrix elements for initial- and final-state radiation. This feature allows a more direct measurement of Higgs boson production through W boson fusion. Second, the same interference also suppresses the dominant multijet non-resonant $b\bar{b}\gamma jj$ background shown in figure 1, improving the expected sensitivity to Higgs boson production. Third, the presence of an isolated high-energy photon can be used to define efficient trigger algorithms for this search.

This paper reports the result of a search for $H\gamma$ production and subsequent $H \rightarrow b\bar{b}$ decay, with a focus on the phase space dominated by the VBF process, using the full Run 2 dataset. In this phase space, the main backgrounds are non-resonant $b\bar{b}\gamma jj$ production and resonant $Z(\rightarrow b\bar{b})\gamma jj$ production. Kinematic event properties are used in a boosted decision tree (BDT) to classify signal and background events, and the BDT output defines a series of increasingly signal-rich event categories. The Higgs boson production rate, defined relative to the SM prediction, is extracted from a simultaneous fit to the Higgs boson candidate mass distribution in multiple event categories.

2 ATLAS detector

The ATLAS experiment [11] at the LHC is a multipurpose particle detector with a cylindrical geometry that covers nearly the entire solid angle around the collision point.¹ It consists of an inner tracking detector surrounded by a thin superconducting solenoid, electromagnetic and hadronic calorimeters, and a muon spectrometer incorporating three large superconducting toroidal magnets.

The inner tracking detector covers the pseudorapidity range $|\eta| < 2.5$. It consists of silicon pixel, silicon microstrip, and transition radiation tracking detectors immersed in a 2 T axial magnetic field. One significant upgrade for the $\sqrt{s} = 13$ TeV run is the insertable B-layer [12, 13], an additional pixel layer close to the interaction point.

The calorimeter system covers the pseudorapidity range $|\eta| < 4.9$. Within the region $|\eta| < 3.2$, electromagnetic calorimetry is provided by barrel and endcap high-granularity lead/liquid-argon (LAr) calorimeters, with an additional thin LAr presampler covering $|\eta| < 1.8$ to correct for energy loss in material upstream of the calorimeters. Hadronic calorimetry is provided by the steel/scintillator-tile calorimeter, segmented into three barrel structures within $|\eta| < 1.7$, and two copper/LAr hadronic endcap calorimeters. The solid angle coverage is completed with forward copper/LAr and tungsten/LAr calorimeter modules optimized for electromagnetic and hadronic measurements, respectively.

The muon spectrometer consists of fast detectors for triggering and high-precision chambers for tracking in a magnetic field generated by superconducting air-core toroids. The field integral of the toroids ranges between 2.0 and 6.0 T m across most of the detector.

A two-level trigger system selects events for offline analysis. Events that match predefined trigger signatures are selected by the first-level trigger system implemented in custom hardware. A subset of those events are selected by software algorithms implemented in the high-level trigger [14]. The first-level trigger accepts events from the 40 MHz bunch crossings at a rate below 100 kHz, and the high-level trigger reduces the rate in order to record events to disk at about 1 kHz.

¹ATLAS uses a right-handed coordinate system with its origin at the nominal interaction point (IP) in the centre of the detector and the z -axis along the beam pipe. The x -axis points from the IP to the centre of the LHC ring, and the y -axis points upwards. Cylindrical coordinates (r, ϕ) are used in the transverse plane, with ϕ being the azimuthal angle around the z -axis. The pseudorapidity is defined in terms of the polar angle θ as $\eta = -\ln \tan(\theta/2)$. The rapidity is defined as $y = 0.5 \ln[(E + p_z)/(E - p_z)]$, where E denotes energy and p_z is the component of the momentum along the beam direction. Angular distance is measured in units of $\Delta R \equiv \sqrt{(\Delta\eta)^2 + (\Delta\phi)^2}$.

3 Data and simulated events

This search uses LHC proton-proton collision data at a centre-of-mass energy of 13 TeV collected with the ATLAS detector from 2015 to 2018. This full Run 2 dataset, with the analysis-specific triggers available, corresponds to an integrated luminosity of 132 fb^{-1} .

Simulated events are used for signal modelling, BDT training, and determining the functional form used to describe the background shape. The $H\gamma jj$ signal events were generated at next-to-leading order (NLO) in α_S with MADGRAPH5_aMC@NLO v2.6.2 [15], using the PDF4LHC15 parton distribution function (PDF) set [16], and passed to HERWIG 7.1 for parton showering and hadronization using parameter values from the HERWIG default tunes [17, 18]. This sample of events can effectively be regarded as VBF $H\gamma$ signal because the contribution from VH production is less than 0.5% of the total after event selection. Higgs boson production from ggF, with Higgs decay into $b\bar{b}$, was simulated at next-to-next-to-leading order with POWHEG-BOX v2 [19–21], using the CT10 PDF set [22] and PYTHIA 8.212 [23] for parton showering and fragmentation with the AZNLO tuned parameter set [24]. Contributions from the $t\bar{t}H$ process are estimated from POWHEG-BOX v2 simulation interfaced with PYTHIA 8.230.

Background events containing two b -jets from the decay of a Z boson, a photon, and two additional jets were generated at leading order (LO) with MADGRAPH5_aMC@NLO v.2.3.3 and PYTHIA 8.210, in separate samples for strong (QCD) and electroweak (EWK) processes. The dominant source of background events is non-resonant QCD production of at least two b -jets, two other jets, and a photon. Even though the contribution from these events is modelled with a functional form, a sample of simulated events is used to train the BDT. This training sample was produced by generating the $b\bar{b}\gamma jj$ final state, excluding diagrams containing on-shell H or Z bosons, at LO with MADGRAPH5_aMC@NLO v2.3.3 using the PDF4LHC15 set of PDFs and interfaced to PYTHIA 8.210 for parton showering and hadronization. The A14 set of tuned parameters was used for the underlying-event description with the NNPDF2.3LO PDF set [25]. A large sample of non-resonant $b\bar{b}\gamma jj$ background events was also produced without parton showering for the background modelling studies described in section 7. For this sample, a parameterized jet energy response function is used to smear the jet transverse energy distribution to match the data.

Certain simulation configurations are common to all samples. The decays of bottom and charm hadrons were performed by EVTGEN [26]. Minimum-bias events were simulated using the PYTHIA 8.210 generator with the NNPDF2.3LO PDF set and the A3 parameter tune [27]. A number of these events, varying in accord with the luminosity profile of the recorded data, were overlaid on the hard-scatter interactions to model pile-up contributions from both the same bunch crossing and neighbouring bunch crossings. The response of the ATLAS detector to the generated events was then modelled using a full simulation of the detector [28] based on GEANT4 [29].

4 Object selection

The event selection builds on standard ATLAS reconstruction algorithms for jets, photons, and leptons. The leptons — electrons and muons — are identified only for the purpose of vetoing events with leptons to preserve orthogonality with other ATLAS measurements.

Jets are reconstructed from three-dimensional positive-energy topological clusters of calorimeter energy deposits calibrated to the electromagnetic scale [30]. These clusters are inputs to the anti- k_t jet reconstruction algorithm [31, 32] with a radius parameter of $R = 0.4$. To suppress jets originating from pile-up vertices, a likelihood-based jet vertex tagger (JVT) [33] is applied to jets with transverse momenta $p_T < 120$ GeV and $|\eta| < 2.5$. A pile-up subtraction algorithm further reduces pile-up contributions to the jet energies [34]. These jet energies are calibrated with MC-derived correction factors, including η -dependent calibrations to ensure consistent jet energy measurements in the central and forward regions of the experiment [34]. The jet energies are further corrected using data-derived calibrations based on the p_T balance between jets and reference objects, such as Z bosons, photons, or high-energy jets.

The MV2c10 multivariate b -tagging algorithm [35] tags b -jets (jets containing b -hadrons) within the tracker acceptance. It uses log-likelihood ratios from two- and three-dimensional impact parameter distributions, secondary and tertiary vertex information, and the jet p_T and η , as inputs to a BDT. The requirement on the BDT output corresponds to a per-jet b -tagging efficiency of 77%, as measured in simulated $t\bar{t}$ events for b -jets with $p_T > 20$ GeV and $|\eta| < 2.5$, and c -jet and light-flavour-jet efficiencies of 25% and 0.9%, respectively. Scale factors are applied to account for efficiency differences between simulated events and data [35–37].

Photon and electron reconstruction begins with clusters of calorimeter energy deposits [38]. Clusters without any matching track or conversion vertex are identified as unconverted photons, while clusters with a matching conversion vertex reconstructed from one or two tracks are identified as converted photons. Clusters with a matching track, re-fitted to account for bremsstrahlung, are identified as electrons. Calorimeter and track information for each photon or electron candidate is used to construct multivariate discriminants for identification, and ‘tight’ selections are applied to both the photons and electrons. To suppress hadronic background, further isolation requirements are optimized with simulated $t\bar{t}$ events [38]. For photon candidates, the calorimeter isolation variable E_T^{iso} is the sum of the transverse energies of topological clusters reconstructed in the electromagnetic and hadronic calorimeters in a cone of size $\Delta R = 0.4$ around the photon candidate, where the $\Delta\eta \times \Delta\phi$ region of size 0.125×0.175 around the photon cluster’s centroid is excluded. The isolation requirement, which depends explicitly on the photon transverse energy E_T^γ , is $E_T^{\text{iso}} < 2.45 \text{ GeV} + 0.022 \times E_T^\gamma$. For electron candidates, both track- and calorimeter-based isolation is required. The track-based isolation requirement is a function of the electron transverse momentum p_T^e and is based on the tracks within a cone of p_T^e -dependent size up to $\Delta R = 0.2$ around the electron candidate [38]. The calorimeter-based isolation requires that the sum of cluster transverse energies within the same ΔR be less than 3.5 GeV.

Muons are reconstructed by combining inner detector tracks, where available, and muon spectrometer tracks up to $|\eta| = 2.7$. They must satisfy the ‘loose’ identification criteria [39]. Identified muons must be isolated from other tracks, with a total summed track p_T less than 1.25 GeV in a cone of $\Delta R = 0.2$ around the muon. Only ‘loose’ muons within the coverage of the inner detector, $|\eta| < 2.5$, are used in this selection.

Overlap between identified photons, leptons, and jets is removed with the following procedure. First, photons within $\Delta R = 0.4$ of any muon or electron are removed. Next, jets within $\Delta R = 0.2$ of any electron are removed, and electrons within $\Delta R = 0.4$ of any remaining jets are removed. Then, jets within $\Delta R = 0.2$ of any muon are removed if fewer than three tracks are associated with the jet or if both $p_T^\mu > 0.5p_T^{\text{jet}}$ and $p_T^\mu > 0.7\sum p_T^{\text{track}}$, where $\sum p_T^{\text{track}}$ is the sum of track transverse momenta associated with the jet. Muons within $\Delta R = \min(0.4, 0.04 + 10 \text{ GeV}/p_T^\mu)$ of any remaining jets are removed. Finally, jets within $\Delta R = 0.4$ of any photon are removed.

5 Event selection

The event selection criteria are based on the object reconstruction algorithms, with additional event-level requirements to select events compatible with VBF $H\gamma$ production. These criteria are similar to the event selection requirements in previous searches [6].

The first-level trigger selection requires an isolated electromagnetic calorimeter object — the photon — with $E_T > 22 \text{ GeV}$. The high-level trigger selects events in the specific VBF-enhanced phase space, defined by the following requirements. An isolated reconstructed photon with $E_T > 25 \text{ GeV}$ is required in addition to at least four jets with $E_T > 35 \text{ GeV}$ and $|\eta| < 4.9$. The requirement that at least one pair of jets in the event has an invariant mass greater than 700 GeV targets the VBF phase space. For most of Run 2, a b -tagging trigger algorithm was used to ensure that at least one jet was b -tagged at the 77% efficiency working point [40].

Additional selection requirements are placed on events that pass the trigger selection. At least one photon with $E_T > 30 \text{ GeV}$ in the regions $|\eta| < 1.37$ or $1.52 < |\eta| < 2.37$ must match the trigger photon. Events must have at least four jets satisfying $p_T > 40 \text{ GeV}$ and $|\eta| < 4.5$, with at least two jets in $|\eta| < 2.5$ passing the b -tagging selection. The two highest- p_T b -tagged jets are assumed to be from the Higgs boson decay; they are identified as $b1$ and $b2$ and at least one of them must match a b -tagged trigger-level jet when the b -tagging trigger algorithm is used. Dedicated b -jet energy corrections are applied to b -tagged jets to improve their energy measurement (scale and resolution) [9]. They equalize the response to jets with semileptonic or hadronic decays of heavy-flavour hadrons and correct for resolution effects. This correction improves the di- b -jet invariant mass m_{bb} resolution by 10%. From the remaining jets, the jet pair with the highest invariant mass is chosen as the VBF jets; they are identified as $j1$ and $j2$. Requiring this invariant mass m_{jj} to be greater than 800 GeV ensures full efficiency for the trigger m_{jj} requirement. Events containing identified and isolated electrons with $p_T > 25 \text{ GeV}$ and $|\eta| < 2.47$ or muons with $p_T > 25 \text{ GeV}$ are vetoed to avoid overlap with other Higgs boson event selections in ATLAS.

Trigger	L1	≥ 1 photon with $E_T > 22$ GeV
	HLT	≥ 1 photon with $E_T > 25$ GeV ≥ 4 jets (or ≥ 3 jets and ≥ 1 b -jet) with $E_T > 35$ GeV and $ \eta < 4.9$ $m_{jj} > 700$ GeV
Offline		≥ 1 photon with $E_T > 30$ GeV and $ \eta < 1.37$ or $1.52 < \eta < 2.37$ ≥ 2 b -jets with $p_T > 40$ GeV and $ \eta < 2.5$ ≥ 2 jets with $p_T > 40$ GeV and $ \eta < 4.5$ $m_{jj} > 800$ GeV $p_T(b\bar{b}) > 60$ GeV No electrons ($p_T > 25$ GeV, $ \eta < 2.47$) or muons ($p_T > 25$ GeV, $ \eta < 2.5$)

Table 1. Trigger and offline event selection criteria for the $H(\rightarrow b\bar{b})\gamma jj$ signature. L1 and HLT refer to the first-level trigger and the high-level trigger, respectively.

The jet p_T requirements in the trigger algorithms and offline event selection can introduce concavity in the m_{bb} distribution, making it more difficult to parameterize with an analytic function. The concavity is removed by requiring the p_T of the di- b -jet system $p_T(b\bar{b})$ to be greater than 60 GeV, a value that was optimized in the large MC sample of non-resonant $b\bar{b}\gamma jj$ background events.

The full list of trigger algorithm and offline event selection requirements, before the event-level BDT classification, is summarized in table 1.

6 Multivariate analysis

An event-level BDT classifies events as being signal-like or background-like, based on a set of kinematic variables selected to optimize the separation. The input variables are chosen to ensure the BDT output discriminant shows low correlation with m_{bb} to prevent distortions of the m_{bb} spectrum. The following variables, ordered by decreasing classification power [41], are used for the BDT training:

1. $\Delta\eta(jj)$, the pseudorapidity difference between the two VBF jets;
2. p_T^{balance} , the transverse momentum balance for selected final-state objects, defined as

$$p_T^{\text{balance}} = \frac{|\vec{p}_T^{b1} + \vec{p}_T^{b2} + \vec{p}_T^{j1} + \vec{p}_T^{j2} + \vec{p}_T^\gamma|}{p_T^{b1} + p_T^{b2} + p_T^{j1} + p_T^{j2} + p_T^\gamma};$$

3. $\Delta R(b1, \gamma)$, the angular distance between the leading b -jet and the photon;
4. m_{jj} , the invariant mass of the two VBF jets;
5. $\Delta R(b2, \gamma)$, the angular distance between the subleading b -jet and the photon;
6. $\text{centrality}(\gamma, j1, j2)$, the rapidity of the photon relative to the VBF jet rapidities, defined as

$$\text{centrality}(\gamma, j1, j2) = \left| \frac{y_\gamma - \frac{y_{j1} + y_{j2}}{2}}{y_{j1} - y_{j2}} \right|;$$

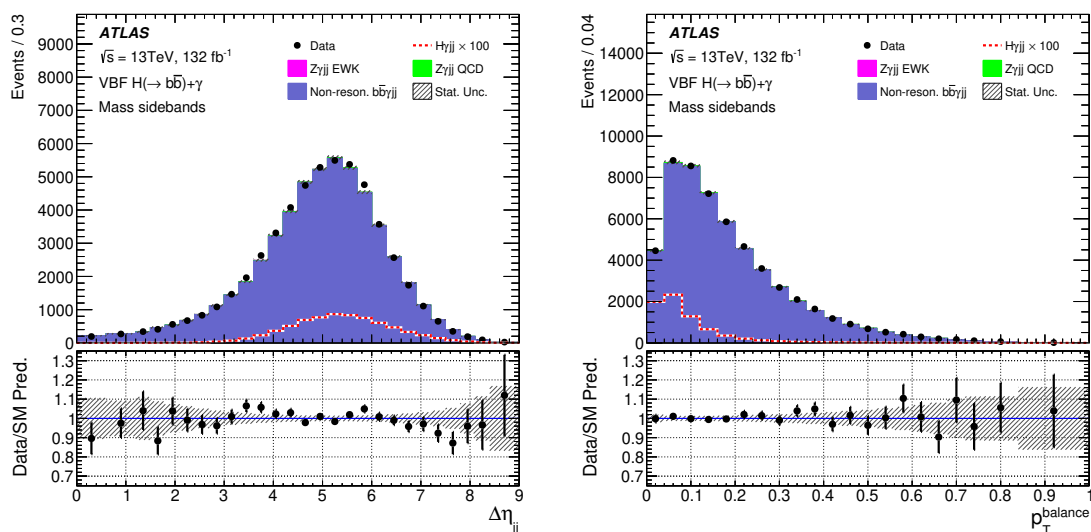


Figure 2. Comparisons of data and simulated event distributions of the BDT input variables $\Delta\eta_{jj}$ (left) and p_T^{balance} (right) in the two m_{bb} sidebands after kinematic reweighting of the non-resonant $b\bar{b}\gamma jj$ background. The data are shown as black points, and the background contributions are stacked in coloured histograms. The Higgs boson signal contribution is scaled up and represented by the dashed red line. The bottom panel in each plot shows the ratio of the data to the SM prediction, where the uncertainty band corresponds to the statistical uncertainty only.

7. $\Delta\phi(b\bar{b}, jj)$, the azimuthal angle difference between the di- b -jet system and the VBF jet system;
8. p_T^{jj} , the transverse momentum of the VBF jets system;
9. $\cos\theta$, the cosine of the angle between the VBF jets plane and b -jets plane in the centre-of-mass frame of the $b\bar{b}jj$ system;² and
10. $\Delta R(b1, j1)$, the angular distance between the leading b -jet and the leading VBF jet.

The $H\gamma jj$ signal sample and the non-resonant $b\bar{b}\gamma jj$ background sample are used for the BDT training in the TMVA package [41]. To improve agreement between the LO non-resonant $b\bar{b}\gamma jj$ simulation and data, analytic correction functions are fit in the mass sidebands ($m_{bb} < 100$ GeV and $m_{bb} > 140$ GeV). They are based on data-to-MC ratios of the distributions for several relevant observables and are used to reweight the simulated events. The overall normalization is also corrected to match the data in the mass sidebands. This procedure is applied sequentially to the distributions of $\Delta\eta_{jj}$, $\min[\Delta R(b1, \gamma), \Delta R(b2, \gamma)]$, and p_T^{balance} , resulting in corrections that are typically less than 10%. The distributions of the other uncorrelated input variables are not significantly affected by the reweighting. Comparisons of the data and MC distributions for the two most powerful classification variables, after the reweighting procedure, are shown in figure 2.

²This angular variable is sensitive to the spin of the particle decaying into $b\bar{b}$. It helps discriminate Higgs boson production from gluon splitting [42].

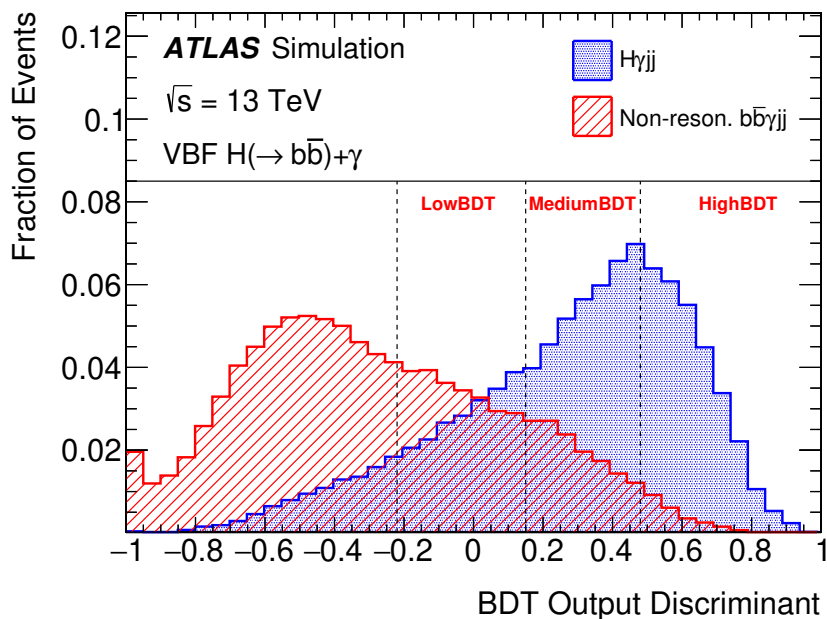


Figure 3. BDT output discriminant distributions for the $H\gamma jj$ signal and non-resonant $b\bar{b}\gamma jj$ background samples. The distributions from the signal and background samples are shown as blue and red hatched histograms, respectively. The vertical dashed lines represent the boundaries of the event categories, defined by the BDT output discriminant.

The BDT output discriminant is used to define three signal categories: HighBDT, MediumBDT, and LowBDT. The boundaries of the three categories are defined sequentially from HighBDT to LowBDT by maximizing the combined VBF Higgs boson signal significance across categories. The BDT output distributions for the signal and background samples within the three categories are shown in figure 3.

7 Signal and background modelling

The main sources of background contributing to the $b\bar{b}\gamma jj$ final-state signature are divided into processes with the decay of a massive gauge boson into b -tagged jet pairs and processes with non-resonant b -tagged jet pairs. The resonant background is dominated by $Z(\rightarrow b\bar{b})\gamma jj$, with a negligible contribution from $W\gamma jj$. The non-resonant background is dominated by multijet $b\bar{b}\gamma jj$ production, with small contributions from $t\bar{t}\gamma$ and single-top events. The expected contributions from the dominant signal and background processes are collected in table 2.

To extract the Higgs boson production rate from fits to data, the signal and dominant backgrounds — the resonant $Z\gamma jj$ and non-resonant $b\bar{b}\gamma jj$ contributions — are parameterized with analytic functions derived from simulated events or data sideband regions. The small contributions from other backgrounds are included in the non-resonant background functions.

Category	LowBDT	MediumBDT	HighBDT
BDT Output	(−0.22, 0.15)	(0.15, 0.48)	(0.48, 1)
VBF+ VH	11.31 ± 0.12	21.07 ± 0.17	18.33 ± 0.15
ggF	1.71 ± 0.41	1.08 ± 0.33	0.19 ± 0.13
$t\bar{t}H$	0.75 ± 0.14	0.19 ± 0.03	0.05 ± 0.01
$Z\gamma jj$ EWK	8.50 ± 0.14	8.91 ± 0.14	5.37 ± 0.11
$Z\gamma jj$ QCD	15.9 ± 1.7	7.2 ± 1.1	1.65 ± 0.52
Non-resonant $b\bar{b}\gamma jj$	2834 \pm 42	1507 \pm 33	322 \pm 17
Expected Yield	2872 \pm 42	1545 \pm 33	348 \pm 17
Data	2964	1522	318

Table 2. Data and expected yields for the Higgs boson signal, resonant $Z\gamma jj$ and non-resonant $b\bar{b}\gamma jj$ background processes, in the three categories defined by the BDT output discriminant. The event yields are calculated from simulated samples in the mass range $100 \text{ GeV} < m_{bb} < 140 \text{ GeV}$. The yields are shown with statistical uncertainties only because experimental and theoretical systematic uncertainties, which depend on fits to data, are an order of magnitude smaller.

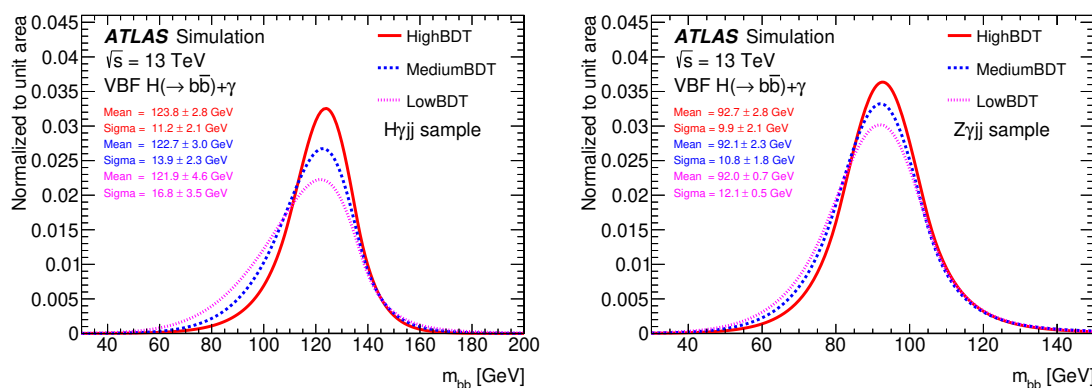


Figure 4. Comparison of the Bukin function parameterizations, normalized to unit area, of the m_{bb} distributions for $H\gamma jj$ events (left) and $Z\gamma jj$ events (right) in the three BDT categories, along with the mean and sigma values for the three fitted functions.

The Higgs boson signal m_{bb} distribution is modelled with a Bukin function [43], parameterized using the simulated samples independently in each of the three event categories defined by the BDT output, as shown in figure 4. Among the possible functions, the Bukin function showed the best fit quality, as gauged by fit residuals across the mass range. With this function, the residuals follow a normal distribution about zero. The resonant $Z\gamma jj$ background is also described with the same Bukin function using independent parameters in each of the three BDT categories.

The model for the non-resonant background is tested and largely determined using the data sidebands outside the mass window $100 \text{ GeV} < m_{bb} < 140 \text{ GeV}$. Several different classes of fitting functions were tested, including polynomial, Bernstein polynomial and

power-law functions. The potential bias arising from the fitting procedure, termed ‘spurious signal’, is estimated by performing signal-plus-background fits over the full mass range in the large simulated sample of non-resonant $b\bar{b}\gamma jj$ background events. The polynomial function, with two terms (first-order) for the HighBDT region or three terms (second-order) for the MediumBDT and LowBDT regions, has the smallest bias among the tested functions and is therefore chosen for the background template in the fit. The standard F -test is used as a confirmation check, assessing the significance of decreases in the reduced χ^2 value as the order of the background-only polynomial fit to the data sidebands is increased. The spurious-signal uncertainty, evaluated separately in each BDT region as the maximum of the fitted spurious signal and the MC statistical uncertainty of the non-resonant $b\bar{b}\gamma jj$ background, is included as a systematic uncertainty in the signal yield. The spurious signal is treated in the same way when $Z\gamma jj$ is treated as signal.

8 Systematic uncertainties

Systematic uncertainties in the Higgs boson production rate arise from choices of modelling and fitting methods — such as the spurious-signal uncertainties — and from uncertainties in the event reconstruction or cross-section calculations. They are summarized in table 3 together with the statistical uncertainties calculated using the methods described in section 9. The systematic uncertainties for the background and signal contributions are divided into experimental and theoretical uncertainties. They affect only the signal and background predictions that are based on simulation; they do not affect the non-resonant background estimate, which is derived from the data only. The uncertainties are propagated through the event selection and the BDT classification to the template distributions. They modify the shape and nominal normalization of the Higgs boson signal process. However, they modify only the shape of the resonant $Z\gamma$ background, as its normalization is derived from the m_{bb} fits in each category separately. In general, the impact of the signal shape uncertainties on the final Higgs boson measurement is smaller than the impact of the experimental systematic uncertainties.

Other uncertainties are related to factors in the full m_{bb} fit, such as the uncertainty in the $Z\gamma$ normalizations (‘ Z boson normalizations’ in table 3). The uncertainties in the $b\bar{b}\gamma jj$ background relate to the fitted shapes (‘Bkg. fit shapes’) and normalizations (‘Bkg. fit normalizations’).

8.1 Experimental uncertainties

The uncertainty in the combined 2015–2018 integrated luminosity is 1.7% [44], obtained using the LUCID-2 detector [45] for the primary luminosity measurements. This uncertainty is applied to all contributions estimated from simulated samples alone.

The dominant jet-related uncertainties for the m_{bb} reconstruction are the jet energy scale (JES) and jet energy resolution (JER) uncertainties. These are determined by p_T -balancing methods in data [34], and the effect on the mass spectrum is determined by shifting or smearing the jet energies before calculating m_{bb} . A total of 8 JER and 30 JES

uncertainty parameters are considered in calculating the effects. The systematic uncertainty in the JVT is estimated by varying the tagger efficiency within its uncertainties. All of these jet uncertainties are summarized in the ‘Jet’ line of table 3.

The uncertainties related to b -tagging jets, covering the trigger-level b -tagging efficiencies and the offline b -tagging efficiency data-to-simulation scale factors, are implemented as variations of the event-weight scale factors. They are determined from data using $t\bar{t}$ events, W boson decays into hadrons, and multijet data [35–37]. The event weight is calculated from the product of the b -tagging scale factors for the two b -jets in the event.

Additional uncertainties are related to the photon energy measurement and reconstruction efficiency [38]. The measurement is only weakly sensitive to the photon energy; therefore a simplified two-parameter model is used to capture the effect of variations in the energy scale and resolution. The efficiency variations considered are due to electromagnetic shower shape variations and isolation calculations. Systematic uncertainties from electron and muon selections are negligible and are therefore ignored.

8.2 Theoretical uncertainties

The theoretical uncertainties on the SM calculations of the total Higgs boson production rates are relevant in the determination of the relative rate of $H\gamma jj$ events compared to the SM expectation. The $H \rightarrow b\bar{b}$ branching ratio uncertainty follows the recommendation of the LHC Higgs Cross Section Working Group, including the uncertainty in the b -quark mass [46]. Cross-section uncertainties due to the choice of renormalization and factorization scales are estimated by varying the choice of both scales up and down by factors of two independently. The largest variation in each BDT classification category is used to define the uncertainty. Similar uncertainties are calculated for the set of PDF variations defined by the eigenvectors of the PDF4LHC15_nlo_mc_pdfas set. The impact on signal normalization is evaluated at the reconstruction level after the event selection, and an overall uncertainty is derived following the PDF4LHC recommendation [16]. Uncertainties in the HERWIG 7 parton shower are estimated by varying the ‘HardScaleFactor’ parameter by factors of two and comparing the resulting acceptances [18].

9 Fit results for Higgs boson production

The Higgs boson signal strength μ_H is defined relative to the total SM prediction for $H\gamma jj$ production, and the VBF signal strength μ_{VBF} is defined relative to the VBF contribution only. They are extracted from an unbinned extended maximum-likelihood fit to the di- b -jet invariant mass distribution in all three BDT classification categories. The likelihood is defined as a product of global Poisson distributions with event-by-event probabilities determined from the signal-plus-background model and the constraints for systematic uncertainties, implemented as nuisance parameters. The nuisance parameters control the effects of the systematic uncertainties and are parameterized by Gaussian or log-normal priors. Each prior’s definition constrains its nuisance parameter to the nominal value within its associated uncertainty.

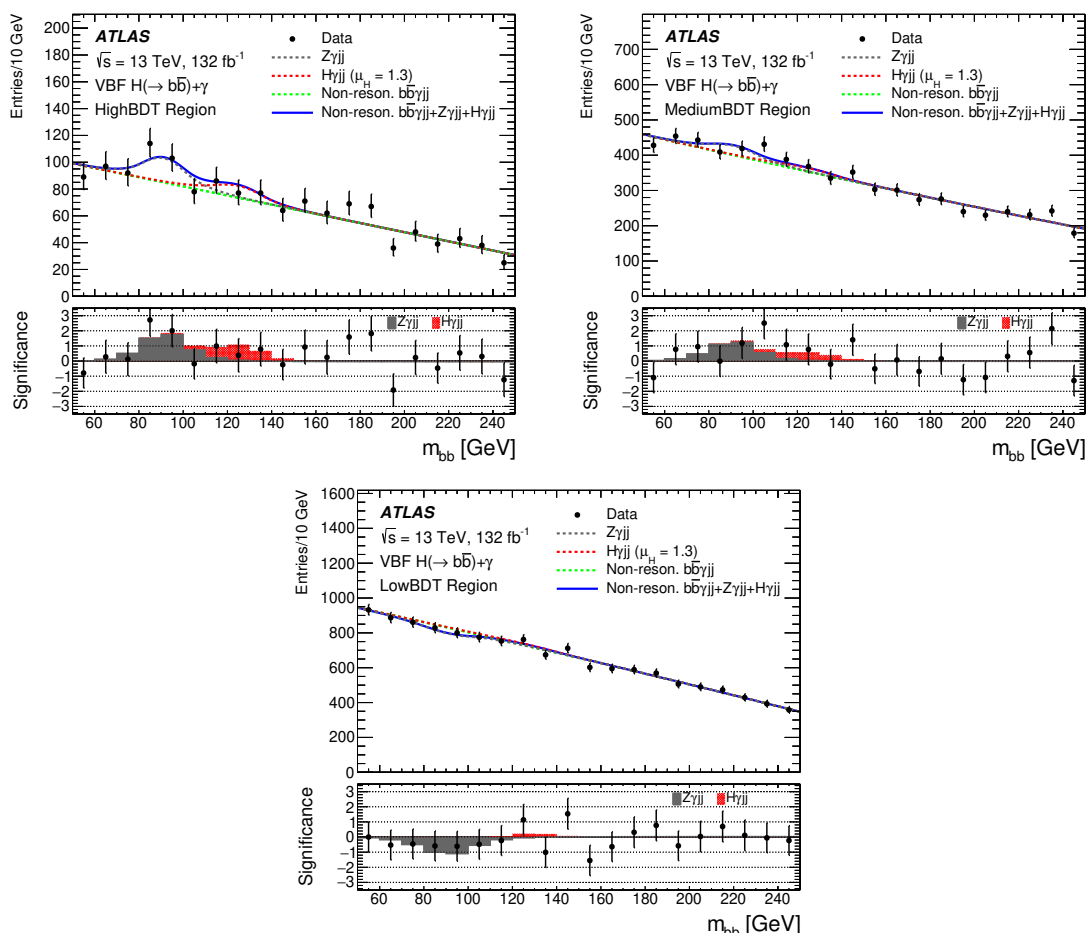


Figure 5. The m_{bb} distributions in the three event categories, overlaid with contributions from the $H\gamma jj$ signal as well as the resonant $Z\gamma jj$ and non-resonant $b\bar{b}\gamma jj$ background fits. The combined χ^2 per degree of freedom is 45.2/45. The bottom panel in each plot presents the significance of the Higgs boson signal relative to the non-resonant $b\bar{b}\gamma jj$ background in each bin, calculated using a Poisson model [47].

The Higgs boson signal strength is the single parameter of interest, common to all three categories, while the $Z\gamma jj$ contribution strength is fit as three separate parameters, uncorrelated across the categories. Using three $Z\gamma jj$ parameters allows for different relative contributions of QCD and EWK processes in the three categories. The uncorrelated parameters describing the non-resonant $b\bar{b}\gamma jj$ background are allowed to float during the fit to obtain the best independent description of the background in each category. The experimental and theoretical uncertainties are correlated across categories during the fit, reflecting their common derivation and calibration. Signal-injection tests, performed by adding simulated signal to the expected background, confirmed the linearity of the fit with no bias in μ_H .

The results of the fits to the m_{bb} distributions in data are shown in figure 5, with contributions from the Higgs boson, Z boson, and background components superimposed.

Source of absolute uncertainty	$\sigma(\mu_H)$ down	$\sigma(\mu_H)$ up
Statistical		
Data statistical	-0.78	+0.80
Bkg. fit shapes	-0.19	+0.22
Bkg. fit normalizations	-0.51	+0.52
Z boson normalizations	-0.15	+0.14
Systematic		
Spurious signal	-0.24	+0.21
Theoretical	-0.01	+0.08
Photon	-0.01	+0.03
Jet	-0.06	+0.20
b -tagging	-0.02	+0.11
Auxiliary	-0.01	+0.04
Total		
Total statistical	-0.96	+0.99
Total systematic	-0.25	+0.32

Table 3. The effect of the uncertainties on the signal strength. The dominant contributions are from the statistical uncertainty of the dataset, background fit uncertainties, and the spurious-signal uncertainty. The statistical uncertainty is calculated by fixing the background fit parameters to their nominal values. Individual uncertainties are then combined to give the total within each group. The small uncertainties from pile-up effects, luminosity measurements, and trigger scale factors are grouped under ‘Auxiliary’ uncertainty.

The inclusive signal strength μ_H and the VBF signal strength μ_{VBF} are both 1.3 ± 1.0 . The similarity of the results is due to the nearly negligible contribution from other Higgs boson production modes in the VBF-enhanced phase space, defined by the high m_{jj} requirement. If the inclusive signal strength is fit as three separate parameters of interest, the results are $\mu_H = 0.7 \pm 1.1, 3.8_{-2.4}^{+2.5}$, and $3.8_{-8.3}^{+7.0}$ in the HighBDT, MediumBDT, and LowBDT categories, respectively.

The Z normalization factors obtained from the fit are $\mu_Z = 1.9 \pm 1.2, 1.5 \pm 1.1$ and $-1.3_{-1.6}^{+1.2}$ in the HighBDT, MediumBDT, and LowBDT categories, respectively. The Z normalization and the μ_H signal strength have a correlation of 15% in the HighBDT category but are uncorrelated in the other categories. If the Z normalization factors are constrained to be non-negative, the change to the combined Higgs boson signal strength μ_H is within rounding errors.

This measurement is consistent with previous results [6]. The dominant uncertainty in the result is the statistical uncertainty of the limited data sample, followed by the background fit uncertainties and the spurious-signal uncertainty. The relative contributions from those and other uncertainties are shown in table 3. Impacts from individual contributions are estimated as the difference in quadrature between the Higgs signal strength uncertainties with each nuisance parameter floating and fixed. The asymmetry observed in some of the systematic uncertainties is due to the limited measurement sensitivity: during the profile likelihood calculation, μ_H can assume values close to 0.

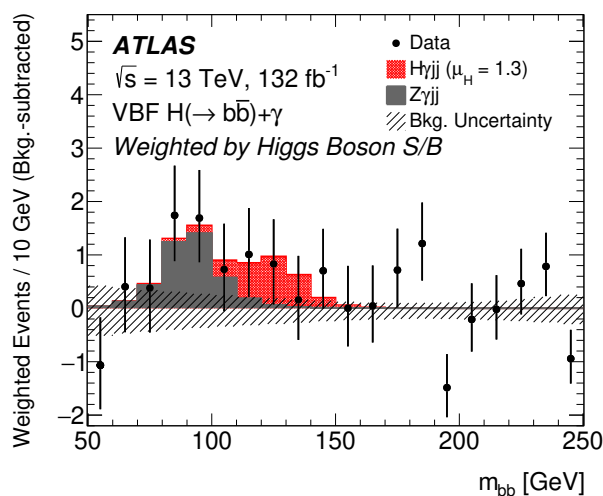


Figure 6. The combined m_{bb} distribution, after subtracting the fitted non-resonant $b\bar{b}\gamma jj$ background, summed over the three BDT categories weighted by S/B in each category, where S and B are the fitted Higgs boson signal yield and $Z\gamma jj + b\bar{b}\gamma jj$ background yield, respectively, calculated in the mass window containing 68% of the Higgs boson signal. The expected contributions of $H\gamma jj$ and $Z\gamma jj$ are also shown, scaled by the fitted Higgs boson signal strength and the $Z\gamma jj$ normalization factors in the three BDT categories. The statistical uncertainty of the fitted non-resonant $b\bar{b}\gamma jj$ background is represented by the hatched band. The statistical uncertainty on data is represented by the error bars on the data points.

The combined mass distribution for the three BDT categories, after the non-resonant $b\bar{b}\gamma jj$ background contribution has been subtracted, is shown in figure 6. The events in each BDT category have been weighted by the signal-to-background ratio S/B , as calculated from the fitted signal and background contributions in the 68% confidence-interval mass window around the Higgs boson signal peak.

10 Conclusion

A search has been conducted for the SM Higgs boson produced in association with a high-energy photon in the $H(\rightarrow b\bar{b})\gamma jj$ signature, with a focus on the phase space typical of vector-boson fusion. The search used the full LHC Run 2 dataset of proton-proton collisions at $\sqrt{s} = 13$ TeV, corresponding to an integrated luminosity of 132 fb^{-1} collected with the ATLAS detector. A BDT is used to separate events into categories, and the m_{bb} distribution is fit to extract the Higgs boson signal production rate. The measured Higgs boson signal strength relative to the SM prediction is $\mu_H = 1.3 \pm 1.0$. This corresponds to an observed signal significance of 1.3 standard deviations, compared to an expected significance of 1.0 standard deviations. The improvement over the previous measurement of $\mu_H = 2.3 \pm 1.8$ comes from the larger dataset, the updated BDT, and more precise Monte Carlo modelling.

Acknowledgments

We thank CERN for the very successful operation of the LHC, as well as the support staff from our institutions without whom ATLAS could not be operated efficiently.

We acknowledge the support of ANPCyT, Argentina; YerPhI, Armenia; ARC, Australia; BMWFW and FWF, Austria; ANAS, Azerbaijan; SSTC, Belarus; CNPq and FAPESP, Brazil; NSERC, NRC and CFI, Canada; CERN; ANID, Chile; CAS, MOST and NSFC, China; COLCIENCIAS, Colombia; MSMT CR, MPO CR and VSC CR, Czech Republic; DNRF and DNSRC, Denmark; IN2P3-CNRS and CEA-DRF/IRFU, France; SRNSFG, Georgia; BMBF, HGF and MPG, Germany; GSRT, Greece; RGC and Hong Kong SAR, China; ISF and Benozziyo Center, Israel; INFN, Italy; MEXT and JSPS, Japan; CNRST, Morocco; NWO, Netherlands; RCN, Norway; MNiSW and NCN, Poland; FCT, Portugal; MNE/IFA, Romania; JINR; MES of Russia and NRC KI, Russian Federation; MESTD, Serbia; MSSR, Slovakia; ARRS and MIZŠ, Slovenia; DST/NRF, South Africa; MICINN, Spain; SRC and Wallenberg Foundation, Sweden; SERI, SNSF and Cantons of Bern and Geneva, Switzerland; MOST, Taiwan; TAEK, Turkey; STFC, United Kingdom; DOE and NSF, United States of America. In addition, individual groups and members have received support from BCKDF, CANARIE, Compute Canada, CRC and IVADO, Canada; Beijing Municipal Science & Technology Commission, China; COST, ERC, ERDF, Horizon 2020 and Marie Skłodowska-Curie Actions, European Union; Investissements d’Avenir Labex, Investissements d’Avenir Idex and ANR, France; DFG and AvH Foundation, Germany; Herakleitos, Thales and Aristeia programmes co-financed by EU-ESF and the Greek NSRF, Greece; BSF-NSF and GIF, Israel; La Caixa Banking Foundation, CERCA Programme Generalitat de Catalunya and PROMETEO and GenT Programmes Generalitat Valenciana, Spain; Göran Gustafssons Stiftelse, Sweden; The Royal Society and Leverhulme Trust, United Kingdom.

The crucial computing support from all WLCG partners is acknowledged gratefully, in particular from CERN, the ATLAS Tier-1 facilities at TRIUMF (Canada), NDGF (Denmark, Norway, Sweden), CC-IN2P3 (France), KIT/GridKA (Germany), INFN-CNAF (Italy), NL-T1 (Netherlands), PIC (Spain), ASGC (Taiwan), RAL (UK) and BNL (USA), the Tier-2 facilities worldwide and large non-WLCG resource providers. Major contributors of computing resources are listed in ref. [48].

Open Access. This article is distributed under the terms of the Creative Commons Attribution License ([CC-BY 4.0](https://creativecommons.org/licenses/by/4.0/)), which permits any use, distribution and reproduction in any medium, provided the original author(s) and source are credited.

References

- [1] ATLAS collaboration, *Observation of a new particle in the search for the Standard Model Higgs boson with the ATLAS detector at the LHC*, *Phys. Lett. B* **716** (2012) 1 [[arXiv:1207.7214](https://arxiv.org/abs/1207.7214)] [[INSPIRE](https://inspirehep.net/literature/1207721)].
- [2] CMS collaboration, *Observation of a New Boson at a Mass of 125 GeV with the CMS Experiment at the LHC*, *Phys. Lett. B* **716** (2012) 30 [[arXiv:1207.7235](https://arxiv.org/abs/1207.7235)] [[INSPIRE](https://inspirehep.net/literature/1207723)].

- [3] E. Gabrielli, F. Maltoni, B. Mele, M. Moretti, F. Piccinini and R. Pittau, *Higgs Boson Production in Association with a Photon in Vector Boson Fusion at the LHC*, *Nucl. Phys. B* **781** (2007) 64 [[hep-ph/0702119](#)] [[INSPIRE](#)].
- [4] E. Gabrielli, B. Mele, F. Piccinini and R. Pittau, *Asking for an extra photon in Higgs production at the LHC and beyond*, *JHEP* **07** (2016) 003 [[arXiv:1601.03635](#)] [[INSPIRE](#)].
- [5] W.H. Furry, *A Symmetry Theorem in the Positron Theory*, *Phys. Rev.* **51** (1937) 125 [[INSPIRE](#)].
- [6] ATLAS collaboration, *Search for Higgs bosons produced via vector-boson fusion and decaying into bottom quark pairs in $\sqrt{s} = 13$ TeV pp collisions with the ATLAS detector*, *Phys. Rev. D* **98** (2018) 052003 [[arXiv:1807.08639](#)] [[INSPIRE](#)].
- [7] ATLAS collaboration, *Combined measurements of Higgs boson production and decay using up to 80 fb^{-1} of proton-proton collision data at $\sqrt{s} = 13$ TeV collected with the ATLAS experiment*, *Phys. Rev. D* **101** (2020) 012002 [[arXiv:1909.02845](#)] [[INSPIRE](#)].
- [8] CMS collaboration, *Combined measurements of Higgs boson couplings in proton-proton collisions at $\sqrt{s} = 13$ TeV*, *Eur. Phys. J. C* **79** (2019) 421 [[arXiv:1809.10733](#)] [[INSPIRE](#)].
- [9] ATLAS collaboration, *Measurements of WH and ZH production in the $H \rightarrow b\bar{b}$ decay channel in pp collisions at 13 TeV with the ATLAS detector*, *Eur. Phys. J. C* **81** (2021) 178 [[arXiv:2007.02873](#)] [[INSPIRE](#)].
- [10] CMS collaboration, *Observation of Higgs boson decay to bottom quarks*, *Phys. Rev. Lett.* **121** (2018) 121801 [[arXiv:1808.08242](#)] [[INSPIRE](#)].
- [11] ATLAS collaboration, *The ATLAS Experiment at the CERN Large Hadron Collider*, 2008 *JINST* **3** S08003 [[INSPIRE](#)].
- [12] ATLAS collaboration, *ATLAS Insertable B-Layer Technical Design Report*, CERN-LHCC-2010-013, ATLAS-TDR-19 (2010).
- [13] ATLAS IBL collaboration, *Production and Integration of the ATLAS Insertable B-Layer*, 2018 *JINST* **13** T05008 [[arXiv:1803.00844](#)] [[INSPIRE](#)].
- [14] ATLAS collaboration, *Performance of the ATLAS Trigger System in 2015*, *Eur. Phys. J. C* **77** (2017) 317 [[arXiv:1611.09661](#)] [[INSPIRE](#)].
- [15] J. Alwall et al., *The automated computation of tree-level and next-to-leading order differential cross sections, and their matching to parton shower simulations*, *JHEP* **07** (2014) 079 [[arXiv:1405.0301](#)] [[INSPIRE](#)].
- [16] J. Butterworth et al., *PDF4LHC recommendations for LHC Run II*, *J. Phys. G* **43** (2016) 023001 [[arXiv:1510.03865](#)] [[INSPIRE](#)].
- [17] M. Bahr et al., *HERWIG++ Physics and Manual*, *Eur. Phys. J. C* **58** (2008) 639 [[arXiv:0803.0883](#)] [[INSPIRE](#)].
- [18] J. Bellm et al., *HERWIG 7.0/HERWIG++ 3.0 release note*, *Eur. Phys. J. C* **76** (2016) 196 [[arXiv:1512.01178](#)] [[INSPIRE](#)].
- [19] P. Nason, *A New method for combining NLO QCD with shower Monte Carlo algorithms*, *JHEP* **11** (2004) 040 [[hep-ph/0409146](#)] [[INSPIRE](#)].
- [20] S. Frixione, P. Nason and C. Oleari, *Matching NLO QCD computations with Parton Shower simulations: the POWHEG method*, *JHEP* **11** (2007) 070 [[arXiv:0709.2092](#)] [[INSPIRE](#)].

- [21] S. Alioli, P. Nason, C. Oleari and E. Re, *A general framework for implementing NLO calculations in shower Monte Carlo programs: the POWHEG BOX*, *JHEP* **06** (2010) 043 [[arXiv:1002.2581](#)] [[INSPIRE](#)].
- [22] H.-L. Lai et al., *New parton distributions for collider physics*, *Phys. Rev. D* **82** (2010) 074024 [[arXiv:1007.2241](#)] [[INSPIRE](#)].
- [23] T. Sjöstrand et al., *An introduction to PYTHIA 8.2*, *Comput. Phys. Commun.* **191** (2015) 159 [[arXiv:1410.3012](#)] [[INSPIRE](#)].
- [24] ATLAS collaboration, *Measurement of the Z/γ^* boson transverse momentum distribution in pp collisions at $\sqrt{s} = 7$ TeV with the ATLAS detector*, *JHEP* **09** (2014) 145 [[arXiv:1406.3660](#)] [[INSPIRE](#)].
- [25] R.D. Ball et al., *Parton distributions with LHC data*, *Nucl. Phys. B* **867** (2013) 244 [[arXiv:1207.1303](#)] [[INSPIRE](#)].
- [26] D.J. Lange, *The EvtGen particle decay simulation package*, *Nucl. Instrum. Meth. A* **462** (2001) 152 [[INSPIRE](#)].
- [27] ATLAS collaboration, *The PYTHIA 8 A3 tune description of ATLAS minimum bias and inelastic measurements incorporating the Donnachie-Landshoff diffractive model*, *ATL-PHYS-PUB-2016-017* (2016).
- [28] ATLAS collaboration, *The ATLAS Simulation Infrastructure*, *Eur. Phys. J. C* **70** (2010) 823 [[arXiv:1005.4568](#)] [[INSPIRE](#)].
- [29] GEANT4 collaboration, *GEANT4 — a simulation toolkit*, *Nucl. Instrum. Meth. A* **506** (2003) 250 [[INSPIRE](#)].
- [30] ATLAS collaboration, *Topological cell clustering in the ATLAS calorimeters and its performance in LHC Run 1*, *Eur. Phys. J. C* **77** (2017) 490 [[arXiv:1603.02934](#)] [[INSPIRE](#)].
- [31] M. Cacciari, G.P. Salam and G. Soyez, *The anti- k_t jet clustering algorithm*, *JHEP* **04** (2008) 063 [[arXiv:0802.1189](#)] [[INSPIRE](#)].
- [32] M. Cacciari, G.P. Salam and G. Soyez, *FastJet User Manual*, *Eur. Phys. J. C* **72** (2012) 1896 [[arXiv:1111.6097](#)] [[INSPIRE](#)].
- [33] *Tagging and suppression of pileup jets with the ATLAS detector*, *ATLAS-CONF-2014-018* (2014).
- [34] ATLAS collaboration, *Jet energy scale and resolution measured in proton-proton collisions at $\sqrt{s} = 13$ TeV with the ATLAS detector*, [arXiv:2007.02645](#) [[INSPIRE](#)].
- [35] ATLAS collaboration, *ATLAS b -jet identification performance and efficiency measurement with $t\bar{t}$ events in pp collisions at $\sqrt{s} = 13$ TeV*, *Eur. Phys. J. C* **79** (2019) 970 [[arXiv:1907.05120](#)] [[INSPIRE](#)].
- [36] ATLAS collaboration, *Measurement of b -tagging Efficiency of c -jets in $t\bar{t}$ Events Using a Likelihood Approach with the ATLAS Detector*, *ATLAS-CONF-2018-001* (2018).
- [37] ATLAS collaboration, *Calibration of light-flavour b -jet mistagging rates using ATLAS proton-proton collision data at $\sqrt{s} = 13$ TeV*, *ATLAS-CONF-2018-006* (2018).
- [38] ATLAS collaboration, *Electron and photon performance measurements with the ATLAS detector using the 2015–2017 LHC proton-proton collision data*, *2019 JINST* **14** P12006 [[arXiv:1908.00005](#)] [[INSPIRE](#)].

- [39] ATLAS collaboration, *Muon reconstruction performance of the ATLAS detector in proton–proton collision data at $\sqrt{s} = 13$ TeV*, *Eur. Phys. J. C* **76** (2016) 292 [[arXiv:1603.05598](#)] [[INSPIRE](#)].
- [40] ATLAS collaboration, *Expected performance of the ATLAS b-tagging algorithms in Run-2*, *ATL-PHYS-PUB-2015-022* (2015).
- [41] A. Hocker et al., *TMVA — Toolkit for Multivariate Data Analysis*, [physics/0703039](#) [[INSPIRE](#)].
- [42] CMS collaboration, *Search for the standard model Higgs boson produced through vector boson fusion and decaying to $b\bar{b}$* , *Phys. Rev. D* **92** (2015) 032008 [[arXiv:1506.01010](#)] [[INSPIRE](#)].
- [43] A.D. Bukin, *Fitting function for asymmetric peaks*, [arXiv:0711.4449](#) [[INSPIRE](#)].
- [44] ATLAS collaboration, *Luminosity determination in pp collisions at $\sqrt{s} = 13$ TeV using the ATLAS detector at the LHC*, *ATLAS-CONF-2019-021* (2019).
- [45] G. Avoni et al., *The new LUCID-2 detector for luminosity measurement and monitoring in ATLAS*, *2018 JINST* **13** P07017 [[INSPIRE](#)].
- [46] LHC HIGGS CROSS SECTION WORKING GROUP collaboration, *Handbook of LHC Higgs Cross Sections: 4. Deciphering the Nature of the Higgs Sector*, [arXiv:1610.07922](#) [[INSPIRE](#)].
- [47] G. Choudalakis and D. Casadei, *Plotting the Differences Between Data and Expectation*, *Eur. Phys. J. Plus* **127** (2012) 25 [[arXiv:1111.2062](#)] [[INSPIRE](#)].
- [48] ATLAS collaboration, *ATLAS Computing Acknowledgements*, *ATL-SOFT-PUB-2020-001* (2020).

The ATLAS collaboration

G. Aad¹⁰¹, B. Abbott¹²⁷, D.C. Abbott¹⁰², A. Abed Abud³⁶, K. Abeling⁵³, D.K. Abhayasinghe⁹³, S.H. Abidi²⁹, O.S. AbouZeid⁴⁰, N.L. Abraham¹⁵⁵, H. Abramowicz¹⁶⁰, H. Abreu¹⁵⁹, Y. Abulaiti⁶, B.S. Acharya^{66a,66b,o}, B. Achkar⁵³, L. Adam⁹⁹, C. Adam Bourdarios⁵, L. Adamczyk^{83a}, L. Adamek¹⁶⁵, J. Adelman¹²⁰, A. Adiguzel^{12c,ad}, S. Adorni⁵⁴, T. Adye¹⁴², A.A. Affolder¹⁴⁴, Y. Afik¹⁵⁹, C. Agapopoulou⁶⁴, M.N. Agaras³⁸, A. Aggarwal¹¹⁸, C. Agheorghiesei^{27c}, J.A. Aguilar-Saavedra^{138f,138a,ac}, A. Ahmad³⁶, F. Ahmadov⁷⁹, W.S. Ahmed¹⁰³, X. Ai¹⁸, G. Aielli^{73a,73b}, S. Akatsuka⁸⁵, M. Akbiyik⁹⁹, T.P.A. Åkesson⁹⁶, E. Akilli⁵⁴, A.V. Akimov¹¹⁰, K. Al Khoury⁶⁴, G.L. Alberghi^{23b,23a}, J. Albert¹⁷⁴, M.J. Alconada Verzini¹⁶⁰, S. Alderweireldt³⁶, M. Aleksa³⁶, I.N. Aleksandrov⁷⁹, C. Alexa^{27b}, T. Alexopoulos¹⁰, A. Alfonsi¹¹⁹, F. Alfonsi^{23b,23a}, M. Alhroob¹²⁷, B. Ali¹⁴⁰, S. Ali¹⁵⁷, M. Aliev¹⁶⁴, G. Alimonti^{68a}, C. Allaire³⁶, B.M.M. Allbrooke¹⁵⁵, P.P. Allport²¹, A. Aloisio^{69a,69b}, F. Alonso⁸⁸, C. Alpigiani¹⁴⁷, E. Alunno Camelia^{73a,73b}, M. Alvarez Estevez⁹⁸, M.G. Alvigi^{69a,69b}, Y. Amaral Coutinho^{80b}, A. Ambler¹⁰³, L. Ambroz¹³³, C. Amelung³⁶, D. Amidei¹⁰⁵, S.P. Amor Dos Santos^{138a}, S. Amoroso⁴⁶, C.S. Amrouche⁵⁴, C. Anastopoulos¹⁴⁸, N. Andari¹⁴³, T. Andeen¹¹, J.K. Anders²⁰, S.Y. Andreato^{45a,45b}, A. Andreazza^{68a,68b}, V. Andrei^{61a}, C.R. Anelli¹⁷⁴, S. Angelidakis⁹, A. Angerami³⁹, A.V. Anisenkov^{121b,121a}, A. Annovi^{71a}, C. Antel⁵⁴, M.T. Anthony¹⁴⁸, E. Antipov¹²⁸, M. Antonelli⁵¹, D.J.A. Antrim¹⁸, F. Anulli^{72a}, M. Aoki⁸¹, J.A. Aparisi Pozo¹⁷², M.A. Aparo¹⁵⁵, L. Aperio Bella⁴⁶, N. Aranzabal³⁶, V. Araujo Ferraz^{80a}, R. Araujo Pereira^{80b}, C. Arcangeletti⁵¹, A.T.H. Arce⁴⁹, J-F. Arguin¹⁰⁹, S. Argyropoulos⁵², J.-H. Arling⁴⁶, A.J. Armbruster³⁶, A. Armstrong¹⁶⁹, O. Arnaez¹⁶⁵, H. Arnold¹¹⁹, Z.P. Arrubarrena Tame¹¹³, G. Artoni¹³³, H. Asada¹¹⁶, K. Asai¹²⁵, S. Asai¹⁶², T. Asawatavonvanich¹⁶³, N. Asbah⁵⁹, E.M. Asimakopoulou¹⁷⁰, L. Asquith¹⁵⁵, J. Assahsah^{35e}, K. Assamagan²⁹, R. Astalos^{28a}, R.J. Atkin^{33a}, M. Atkinson¹⁷¹, N.B. Atlay¹⁹, H. Atmani⁶⁴, P.A. Atmasiddha¹⁰⁵, K. Augsten¹⁴⁰, V.A. Austrup¹⁸⁰, G. Avolio³⁶, M.K. Ayoub^{15c}, G. Azuelos^{109,ak}, D. Babal^{28a}, H. Bachacou¹⁴³, K. Bachas¹⁶¹, F. Backman^{45a,45b}, P. Bagnaia^{72a,72b}, M. Bahmani⁸⁴, H. Bahrasemani¹⁵¹, A.J. Bailey¹⁷², V.R. Bailey¹⁷¹, J.T. Baines¹⁴², C. Bakalis¹⁰, O.K. Baker¹⁸¹, P.J. Bakker¹¹⁹, E. Bakos¹⁶, D. Bakshi Gupta⁸, S. Balaji¹⁵⁶, R. Balasubramanian¹¹⁹, E.M. Baldin^{121b,121a}, P. Balek¹⁷⁸, F. Balli¹⁴³, W.K. Balunas¹³³, J. Balz⁹⁹, E. Banas⁸⁴, M. Bandieramonte¹³⁷, A. Bandyopadhyay¹⁹, L. Barak¹⁶⁰, W.M. Barbe³⁸, E.L. Barberio¹⁰⁴, D. Barberis^{55b,55a}, M. Barbero¹⁰¹, G. Barbour⁹⁴, T. Barillari¹¹⁴, M-S. Barisits³⁶, J. Barkeloo¹³⁰, T. Barklow¹⁵², B.M. Barnett¹⁴², R.M. Barnett¹⁸, Z. Barnovska-Blenessy^{60a}, A. Baroncelli^{60a}, G. Barone²⁹, A.J. Barr¹³³, L. Barranco Navarro^{45a,45b}, F. Barreiro⁹⁸, J. Barreiro Guimarães da Costa^{15a}, U. Barron¹⁶⁰, S. Barsov¹³⁶, F. Bartels^{61a}, R. Bartoldus¹⁵², G. Bartolini¹⁰¹, A.E. Barton⁸⁹, P. Bartos^{28a}, A. Basalae⁴⁶, A. Basan⁹⁹, A. Bassalat^{64,ah}, M.J. Basso¹⁶⁵, C.R. Basson¹⁰⁰, R.L. Bates⁵⁷, S. Batlamous^{35f}, J.R. Batley³², B. Batool¹⁵⁰, M. Battaglia¹⁴⁴, M. Bauc^{72a,72b}, F. Bauer^{143,*}, P. Bauer²⁴, H.S. Bawa³¹, A. Bayirli^{12c}, J.B. Beacham⁴⁹, T. Beau¹³⁴, P.H. Beauchemin¹⁶⁸, F. Becherer⁵², P. Bechtel²⁴, H.P. Beck^{20,q}, K. Becker¹⁷⁶, C. Becot⁴⁶, A. Beddall^{12d}, A.J. Beddall^{12a}, V.A. Bednyakov⁷⁹, C.P. Bee¹⁵⁴, T.A. Beermann¹⁸⁰, M. Begalli^{80b}, M. Begel²⁹, A. Behara¹⁵⁴, J.K. Behr⁴⁶, F. Beisiegel²⁴, M. Belfkir⁵, G. Bella¹⁶⁰, L. Bellagamba^{23b}, A. Bellerive³⁴, P. Bellos²¹, K. Beloborodov^{121b,121a}, K. Belotskiy¹¹¹, N.L. Belyaev¹¹¹, D. Benchekroun^{35a}, N. Benekos¹⁰, Y. Benhammou¹⁶⁰, D.P. Benjamin⁶, M. Benoit²⁹, J.R. Bensinger²⁶, S. Bentvelsen¹¹⁹, L. Beresford¹³³, M. Beretta⁵¹, D. Berge¹⁹, E. Bergeas Kuutmann¹⁷⁰, N. Berger⁵, B. Bergmann¹⁴⁰, L.J. Bergsten²⁶, J. Beringer¹⁸, S. Berlendis⁷, G. Bernardi¹³⁴, C. Bernius¹⁵², F.U. Bernlochner²⁴, T. Berry⁹³, P. Berta⁹⁹, A. Berthold⁴⁸, I.A. Bertram⁸⁹, O. Bessidskaia Bylund¹⁸⁰, S. Bethke¹¹⁴, A. Betti⁴², A.J. Bevan⁹², S. Bhatta¹⁵⁴, D.S. Bhattacharya¹⁷⁵, P. Bhattarai²⁶, V.S. Bhopatkar⁶, R. Bi¹³⁷, R.M. Bianchi¹³⁷,

O. Biebel¹¹³, D. Biedermann¹⁹, R. Bielski³⁶, K. Bierwagen⁹⁹, N.V. Biesuz^{71a,71b}, M. Biglietti^{74a}, T.R.V. Billoud¹⁴⁰, M. Bindi⁵³, A. Bingul^{12d}, C. Bini^{72a,72b}, S. Biondi^{23b,23a}, C.J. Birch-sykes¹⁰⁰, M. Birman¹⁷⁸, T. Bisanz³⁶, J.P. Biswal³, D. Biswas^{179,j}, A. Bitadze¹⁰⁰, C. Bittrich⁴⁸, K. Bjørke¹³², T. Blazek^{28a}, I. Bloch⁴⁶, C. Blocker²⁶, A. Blue⁵⁷, U. Blumenschein⁹², G.J. Bobbink¹¹⁹, V.S. Bobrovnikov^{121b,121a}, D. Bogavac¹⁴, A.G. Bogdanchikov^{121b,121a}, C. Bohm^{45a}, V. Boisvert⁹³, P. Bokan^{170,53}, T. Bold^{83a}, M. Bomben¹³⁴, M. Bona⁹², J.S. Bonilla¹³⁰, M. Boonekamp¹⁴³, C.D. Booth⁹³, A.G. Borbély⁵⁷, H.M. Borecka-Bielska⁹⁰, L.S. Borgna⁹⁴, A. Borisov¹²², G. Borissov⁸⁹, D. Bortoletto¹³³, D. Boscherini^{23b}, M. Bosman¹⁴, J.D. Bossio Sola¹⁰³, K. Bouaouda^{35a}, J. Boudreau¹³⁷, E.V. Bouhova-Thacker⁸⁹, D. Boumediene³⁸, R. Bouquet¹³⁴, A. Boveia¹²⁶, J. Boyd³⁶, D. Boye^{33c}, I.R. Boyko⁷⁹, A.J. Bozson⁹³, J. Bracinik²¹, N. Brahimi^{60d,60c}, G. Brandt¹⁸⁰, O. Brandt³², F. Braren⁴⁶, B. Brau¹⁰², J.E. Brau¹³⁰, W.D. Breaden Madden⁵⁷, K. Brendlinger⁴⁶, R. Brenner¹⁵⁹, L. Brenner³⁶, R. Brenner¹⁷⁰, S. Bressler¹⁷⁸, B. Brickwedde⁹⁹, D.L. Briglin²¹, D. Britton⁵⁷, D. Britzger¹¹⁴, I. Brock²⁴, R. Brock¹⁰⁶, G. Brooijmans³⁹, W.K. Brooks^{145d}, E. Brost²⁹, P.A. Bruckman de Renstrom⁸⁴, B. Brüers⁴⁶, D. Bruncko^{28b}, A. Bruni^{23b}, G. Bruni^{23b}, M. Bruschi^{23b}, N. Brusino^{72a,72b}, L. Bryngemark¹⁵², T. Buanes¹⁷, Q. Buat¹⁵⁴, P. Buchholz¹⁵⁰, A.G. Buckley⁵⁷, I.A. Budagov⁷⁹, M.K. Bugge¹³², O. Bulekov¹¹¹, B.A. Bullard⁵⁹, T.J. Burch¹²⁰, S. Burdin⁹⁰, C.D. Burgard⁴⁶, A.M. Burger¹²⁸, B. Burghgrave⁸, J.T.P. Burr⁴⁶, C.D. Burton¹¹, J.C. Burzynski¹⁰², V. Büscher⁹⁹, E. Buschmann⁵³, P.J. Bussey⁵⁷, J.M. Butler²⁵, C.M. Buttar⁵⁷, J.M. Butterworth⁹⁴, W. Buttinger¹⁴², C.J. Buxo Vazquez¹⁰⁶, A.R. Buzykaev^{121b,121a}, G. Cabras^{23b,23a}, S. Cabrera Urbán¹⁷², D. Caforio⁵⁶, H. Cai¹³⁷, V.M.M. Cairo¹⁵², O. Cakir^{4a}, N. Calace³⁶, P. Calafiura¹⁸, G. Calderini¹³⁴, P. Calfayan⁶⁵, G. Callea⁵⁷, L.P. Caloba^{80b}, A. Caltabiano^{73a,73b}, S. Calvente Lopez⁹⁸, D. Calvet³⁸, S. Calvet³⁸, T.P. Calvet¹⁰¹, M. Calvetti^{71a,71b}, R. Camacho Toro¹³⁴, S. Camarda³⁶, D. Camarero Munoz⁹⁸, P. Camarri^{73a,73b}, M.T. Camerlingo^{74a,74b}, D. Cameron¹³², C. Camincher³⁶, S. Campana³⁶, M. Campanelli⁹⁴, A. Camplani⁴⁰, V. Canale^{69a,69b}, A. Canesse¹⁰³, M. Cano Bret⁷⁷, J. Cantero¹²⁸, Y. Cao¹⁷¹, M. Capua^{41b,41a}, R. Cardarelli^{73a}, F. Cardillo¹⁷², G. Carducci^{41b,41a}, T. Carli³⁶, G. Carlino^{69a}, B.T. Carlson¹³⁷, E.M. Carlson^{174,166a}, L. Carminati^{68a,68b}, R.M.D. Carney¹⁵², S. Caron¹¹⁸, E. Carquin^{145d}, S. Carrá⁴⁶, G. Carratta^{23b,23a}, J.W.S. Carter¹⁶⁵, T.M. Carter⁵⁰, M.P. Casado^{14,g}, A.F. Casha¹⁶⁵, E.G. Castiglia¹⁸¹, F.L. Castillo¹⁷², L. Castillo Garcia¹⁴, V. Castillo Gimenez¹⁷², N.F. Castro^{138a,138e}, A. Catinaccio³⁶, J.R. Catmore¹³², A. Cattai³⁶, V. Cavaliere²⁹, V. Cavasinni^{71a,71b}, E. Celebi^{12b}, F. Celli¹³³, K. Cerny¹²⁹, A.S. Cerqueira^{80a}, A. Cerri¹⁵⁵, L. Cerrito^{73a,73b}, F. Cerutti¹⁸, A. Cervelli^{23b,23a}, S.A. Cetin^{12b}, Z. Chadi^{35a}, D. Chakraborty¹²⁰, J. Chan¹⁷⁹, W.S. Chan¹¹⁹, W.Y. Chan⁹⁰, J.D. Chapman³², B. Chargeishvili^{158b}, D.G. Charlton²¹, T.P. Charman⁹², M. Chatterjee²⁰, C.C. Chau³⁴, S. Chekanov⁶, S.V. Chekulaev^{166a}, G.A. Chelkov^{79,af}, B. Chen⁷⁸, C. Chen^{60a}, C.H. Chen⁷⁸, H. Chen^{15c}, H. Chen²⁹, J. Chen^{60a}, J. Chen³⁹, J. Chen²⁶, S. Chen¹³⁵, S.J. Chen^{15c}, X. Chen^{15b}, Y. Chen^{60a}, Y-H. Chen⁴⁶, H.C. Cheng^{62a}, H.J. Cheng^{15a}, A. Cheplakov⁷⁹, E. Cheremushkina¹²², R. Cherkou El Moursli^{35f}, E. Cheu⁷, K. Cheung⁶³, T.J.A. Chevalérias¹⁴³, L. Chevalier¹⁴³, V. Chiarella⁵¹, G. Chiarelli^{71a}, G. Chiodini^{67a}, A.S. Chisholm²¹, A. Chitan^{27b}, I. Chiu¹⁶², Y.H. Chiu¹⁷⁴, M.V. Chizhov⁷⁹, K. Choi¹¹, A.R. Chomont^{72a,72b}, Y. Chou¹⁰², Y.S. Chow¹¹⁹, L.D. Christopher^{33e}, M.C. Chu^{62a}, X. Chu^{15a,15d}, J. Chudoba¹³⁹, J.J. Chwastowski⁸⁴, D. Cieri¹¹⁴, K.M. Ciesla⁸⁴, V. Cindro⁹¹, I.A. Cioară^{27b}, A. Ciocio¹⁸, F. Ciotto^{69a,69b}, Z.H. Citron^{178,k}, M. Citterio^{68a}, D.A. Ciubotaru^{27b}, B.M. Ciungu¹⁶⁵, A. Clark⁵⁴, P.J. Clark⁵⁰, S.E. Clawson¹⁰⁰, C. Clement^{45a,45b}, L. Clissa^{23b,23a}, Y. Coadou¹⁰¹, M. Cobal^{66a,66c}, A. Coccaro^{55b}, J. Cochran⁷⁸, R. Coelho Lopes De Sa¹⁰², H. Cohen¹⁶⁰, A.E.C. Coimbra³⁶, B. Cole³⁹, A.P. Colijn¹¹⁹, J. Collot⁵⁸, P. Conde Muiño^{138a,138h}, S.H. Connell^{33c}, I.A. Connelly⁵⁷, F. Conventi^{69a,al}, A.M. Cooper-Sarkar¹³³, F. Cormier¹⁷³, L.D. Corpe⁹⁴, M. Corradi^{72a,72b}, E.E. Corrigan⁹⁶, F. Corriveau^{103,aa}, M.J. Costa¹⁷², F. Costanza⁵, D. Costanzo¹⁴⁸, G. Cowan⁹³, J.W. Cowley³²,

J. Crane¹⁰⁰, K. Cranmer¹²⁴, R.A. Creager¹³⁵, S. Crépe-Renaudin⁵⁸, F. Crescioli¹³⁴,
 M. Cristinziani²⁴, M. Cristoforetti^{75a,75b}, V. Croft¹⁶⁸, G. Crosetti^{41b,41a}, A. Cueto⁵,
 T. Cuhadar Donszelmann¹⁶⁹, H. Cui^{15a,15d}, A.R. Cukierman¹⁵², W.R. Cunningham⁵⁷,
 S. Czekierda⁸⁴, P. Czodrowski³⁶, M.M. Czurylo^{61b}, M.J. Da Cunha Sargedas De Sousa^{60b},
 J.V. Da Fonseca Pinto^{80b}, C. Da Via¹⁰⁰, W. Dabrowski^{83a}, F. Dachs³⁶, T. Dado⁴⁷, S. Dahbi^{33e},
 T. Dai¹⁰⁵, C. Dallapiccola¹⁰², M. Dam⁴⁰, G. D'amen²⁹, V. D'Amico^{74a,74b}, J. Damp⁹⁹,
 J.R. Dandoy¹³⁵, M.F. Daneri³⁰, M. Danninger¹⁵¹, V. Dao³⁶, G. Darbo^{55b}, O. Dartsis⁵,
 A. Dattagupta¹³⁰, S. D'Auria^{68a,68b}, C. David^{166b}, T. Davidek¹⁴¹, D.R. Davis⁴⁹, I. Dawson¹⁴⁸,
 K. De⁸, R. De Asmundis^{69a}, M. De Beurs¹¹⁹, S. De Castro^{23b,23a}, N. De Groot¹¹⁸, P. de Jong¹¹⁹,
 H. De la Torre¹⁰⁶, A. De Maria^{15c}, D. De Pedis^{72a}, A. De Salvo^{72a}, U. De Sanctis^{73a,73b},
 M. De Santis^{73a,73b}, A. De Santo¹⁵⁵, J.B. De Vivie De Regie⁵⁸, D.V. Dedovich⁷⁹, A.M. Deiana⁴²,
 J. Del Peso⁹⁸, Y. Delabat Diaz⁴⁶, D. Delgove⁶⁴, F. Deliot¹⁴³, C.M. Delitzsch⁷,
 M. Della Pietra^{69a,69b}, D. Della Volpe⁵⁴, A. Dell'Acqua³⁶, L. Dell'Asta^{73a,73b}, M. Delmastro⁵,
 C. Delporte⁶⁴, P.A. Delsart⁵⁸, S. Demers¹⁸¹, M. Demichev⁷⁹, G. Demontigny¹⁰⁹, S.P. Denisov¹²²,
 L. D'Eramo¹²⁰, D. Derendarz⁸⁴, J.E. Derkaoui^{35e}, F. Derue¹³⁴, P. Dervan⁹⁰, K. Desch²⁴,
 K. Dette¹⁶⁵, C. Deutsch²⁴, P.O. Deviveiros³⁶, F.A. Di Bello^{72a,72b}, A. Di Ciaccio^{73a,73b},
 L. Di Ciaccio⁵, C. Di Donato^{69a,69b}, A. Di Girolamo³⁶, G. Di Gregorio^{71a,71b}, A. Di Luca^{75a,75b},
 B. Di Micco^{74a,74b}, R. Di Nardo^{74a,74b}, R. Di Sipio¹⁶⁵, C. Diaconu¹⁰¹, F.A. Dias¹¹⁹,
 T. Dias Do Vale^{138a}, M.A. Diaz^{145a}, F.G. Diaz Capriles²⁴, J. Dickinson¹⁸, M. Didenko¹⁶⁴,
 E.B. Diehl¹⁰⁵, J. Dietrich¹⁹, S. Díez Cornell⁴⁶, C. Diez Pardos¹⁵⁰, A. Dimitrievska¹⁸, W. Ding^{15b},
 J. Dingfelder²⁴, S.J. Dittmeier^{61b}, F. Dittus³⁶, F. Djama¹⁰¹, T. Djobava^{158b}, J.I. Djuvsland¹⁷,
 M.A.B. Do Vale¹⁴⁶, M. Dobre^{27b}, D. Dodsworth²⁶, C. Doglioni⁹⁶, J. Dolejsi¹⁴¹, Z. Dolezal¹⁴¹,
 M. Donadelli^{80c}, B. Dong^{60c}, J. Donini³⁸, A. D'onofrio^{15c}, M. D'Onofrio⁹⁰, J. Dopke¹⁴²,
 A. Doria^{69a}, M.T. Dova⁸⁸, A.T. Doyle⁵⁷, E. Drechsler¹⁵¹, E. Dreyer¹⁵¹, T. Dreyer⁵³,
 A.S. Drobac¹⁶⁸, D. Du^{60b}, T.A. du Pree¹¹⁹, Y. Duan^{60d}, F. Dubinin¹¹⁰, M. Dubovsky^{28a},
 A. Dubreuil⁵⁴, E. Duchovni¹⁷⁸, G. Duckeck¹¹³, O.A. Ducu^{36,27b}, D. Duda¹¹⁴, A. Dudarev³⁶,
 A.C. Dudder⁹⁹, M. D'uffizi¹⁰⁰, L. Duflot⁶⁴, M. Dührssen³⁶, C. Dülsen¹⁸⁰, M. Dumancic¹⁷⁸,
 A.E. Dumitriu^{27b}, M. Dunford^{161a}, S. Dungs⁴⁷, A. Duperrin¹⁰¹, H. Duran Yildiz^{4a}, M. Düren⁵⁶,
 A. Durglishvili^{158b}, B. Dutta⁴⁶, D. Duvnjak¹, G.I. Dyckes¹³⁵, M. Dyndal³⁶, S. Dysch¹⁰⁰,
 B.S. Dziedzic⁸⁴, M.G. Eggleston⁴⁹, T. Eifert⁸, G. Eigen¹⁷, K. Einsweiler¹⁸, T. Ekelof¹⁷⁰,
 H. El Jarrari^{35f}, V. EllaJosyula¹⁷⁰, M. Ellert¹⁷⁰, F. Ellinghaus¹⁸⁰, A.A. Elliot⁹², N. Ellis³⁶,
 J. Elmsheuser²⁹, M. Elsing³⁶, D. Emeliyanov¹⁴², A. Emerman³⁹, Y. Enari¹⁶², J. Erdmann⁴⁷,
 A. Ereditato²⁰, P.A. Erland⁸⁴, M. Errenst¹⁸⁰, M. Escalier⁶⁴, C. Escobar¹⁷², O. Estrada Pastor¹⁷²,
 E. Etzion¹⁶⁰, G. Evans^{138a}, H. Evans⁶⁵, M.O. Evans¹⁵⁵, A. Ezhilov¹³⁶, F. Fabbri⁵⁷,
 L. Fabbri^{23b,23a}, V. Fabiani¹¹⁸, G. Facini¹⁷⁶, R.M. Fakhrutdinov¹²², S. Falciano^{72a}, P.J. Falke²⁴,
 S. Falke³⁶, J. Faltova¹⁴¹, Y. Fang^{15a}, Y. Fang^{15a}, G. Fanourakis⁴⁴, M. Fanti^{68a,68b}, M. Faraj^{60c},
 A. Farbin⁸, A. Farilla^{74a}, E.M. Farina^{70a,70b}, T. Farooque¹⁰⁶, S.M. Farrington⁵⁰, P. Farthouat³⁶,
 F. Fassi^{35f}, P. Fassnacht³⁶, D. Fassouliotis⁹, M. Fauci Giannelli⁵⁰, W.J. Fawcett³², L. Fayard⁶⁴,
 O.L. Fedin^{136,p}, A. Fehr²⁰, M. Feickert¹⁷¹, L. Felgioni¹⁰¹, A. Fell¹⁴⁸, C. Feng^{60b}, M. Feng⁴⁹,
 M.J. Fenton¹⁶⁹, A.B. Fenyuk¹²², S.W. Ferguson⁴³, J. Ferrando⁴⁶, A. Ferrari¹⁷⁰, P. Ferrari¹¹⁹,
 R. Ferrari^{70a}, A. Ferrer¹⁷², D. Ferrere⁵⁴, C. Ferretti¹⁰⁵, F. Fiedler⁹⁹, A. Filipčić⁹¹, F. Filthaut¹¹⁸,
 K.D. Finelli²⁵, M.C.N. Fiolhais^{138a,138c,a}, L. Fiorini¹⁷², F. Fischer¹¹³, J. Fischer⁹⁹, W.C. Fisher¹⁰⁶,
 T. Fitschen²¹, I. Fleck¹⁵⁰, P. Fleischmann¹⁰⁵, T. Flick¹⁸⁰, B.M. Flierl¹¹³, L. Flores¹³⁵,
 L.R. Flores Castillo^{62a}, F.M. Follega^{75a,75b}, N. Fomin¹⁷, J.H. Foo¹⁶⁵, G.T. Forcolin^{75a,75b},
 B.C. Forland⁶⁵, A. Formica¹⁴³, F.A. Förster¹⁴, A.C. Forti¹⁰⁰, E. Fortin¹⁰¹, M.G. Foti¹³³,
 D. Fournier⁶⁴, H. Fox⁸⁹, P. Francavilla^{71a,71b}, S. Francescato^{72a,72b}, M. Franchini^{23b,23a},
 S. Franchino^{61a}, D. Francis³⁶, L. Franco⁵, L. Franconi²⁰, M. Franklin⁵⁹, G. Frattari^{72a,72b},
 P.M. Freeman²¹, B. Freund¹⁰⁹, W.S. Freund^{80b}, E.M. Freundlich⁴⁷, D.C. Frizzell¹²⁷,

D. Froidevaux³⁶, J.A. Frost¹³³, M. Fujimoto¹²⁵, E. Fullana Torregrosa¹⁷², T. Fusayasu¹¹⁵,
 J. Fuster¹⁷², A. Gabrielli^{23b,23a}, A. Gabrielli³⁶, P. Gadow¹¹⁴, G. Gagliardi^{55b,55a}, L.G. Gagnon¹⁰⁹,
 G.E. Gallardo¹³³, E.J. Gallas¹³³, B.J. Gallop¹⁴², R. Gamboa Goni⁹², K.K. Gan¹²⁶, S. Ganguly¹⁷⁸,
 J. Gao^{60a}, Y. Gao⁵⁰, Y.S. Gao^{31,m}, F.M. Garay Walls^{145a}, C. García¹⁷², J.E. García Navarro¹⁷²,
 J.A. García Pascual^{15a}, M. Garcia-Sciveres¹⁸, R.W. Gardner³⁷, S. Gargiulo⁵², C.A. Garner¹⁶⁵,
 V. Garonne¹³², S.J. Gasiorowski¹⁴⁷, P. Gaspar^{80b}, G. Gaudio^{70a}, P. Gauzzi^{72a,72b},
 I.L. Gavrilenko¹¹⁰, A. Gavrilyuk¹²³, C. Gay¹⁷³, G. Gaycken⁴⁶, E.N. Gazis¹⁰, A.A. Geanta^{27b},
 C.M. Gee¹⁴⁴, C.N.P. Gee¹⁴², J. Geisen⁹⁶, M. Geisen⁹⁹, C. Gemme^{55b}, M.H. Genest⁵⁸, C. Geng¹⁰⁵,
 S. Gentile^{72a,72b}, S. George⁹³, T. Geralis⁴⁴, L.O. Gerlach⁵³, P. Gessinger-Befurt⁹⁹, G. Gessner⁴⁷,
 M. Ghasemi Bostanabad¹⁷⁴, M. Ghneimat¹⁵⁰, A. Ghosh⁶⁴, A. Ghosh⁷⁷, B. Giacobbe^{23b},
 S. Giagu^{72a,72b}, N. Giangiacomi¹⁶⁵, P. Giannetti^{71a}, A. Giannini^{69a,69b}, G. Giannini¹⁴,
 S.M. Gibson⁹³, M. Gignac¹⁴⁴, D.T. Gil^{83b}, B.J. Gilbert³⁹, D. Gillberg³⁴, G. Gilles¹⁸⁰,
 N.E.K. Gillwald⁴⁶, D.M. Gingrich^{3,ak}, M.P. Giordani^{66a,66c}, P.F. Giraud¹⁴³, G. Giugliarelli^{66a,66c},
 D. Giugni^{68a}, F. Giuli^{73a,73b}, S. Gkaitatzis¹⁶¹, I. Gkialas^{9,h}, E.L. Gkougkousis¹⁴,
 P. Gkoutoumis¹⁰, L.K. Gladilin¹¹², C. Glasman⁹⁸, P.C.F. Glaysher⁴⁶, G.R. Gledhill¹³⁰,
 I. Gnesi^{41b,c}, M. Goblirsch-Kolb²⁶, D. Godin¹⁰⁹, S. Goldfarb¹⁰⁴, T. Golling⁵⁴, D. Golubkov¹²²,
 A. Gomes^{138a,138b}, R. Goncalves Gama⁵³, R. Gonçalo^{138a,138c}, G. Gonella¹³⁰, L. Gonella²¹,
 A. Gongadze⁷⁹, F. Gonnella²¹, J.L. Gonski³⁹, S. González de la Hoz¹⁷², S. Gonzalez Fernandez¹⁴,
 R. Gonzalez Lopez⁹⁰, C. Gonzalez Renteria¹⁸, R. Gonzalez Suarez¹⁷⁰, S. Gonzalez-Sevilla⁵⁴,
 G.R. Gonzalvo Rodriguez¹⁷², L. Goossens³⁶, N.A. Gorasia²¹, P.A. Gorbounov¹²³, H.A. Gordon²⁹,
 B. Gorini³⁶, E. Gorini^{67a,67b}, A. Gorišek⁹¹, A.T. Goshaw⁴⁹, M.I. Gostkin⁷⁹, C.A. Gottardo¹¹⁸,
 M. Gouighri^{35b}, A.G. Goussiou¹⁴⁷, N. Govender^{33c}, C. Goy⁵, I. Grabowska-Bold^{83a},
 E. Gramstad¹³², S. Grancagnolo¹⁹, M. Grandi¹⁵⁵, V. Gratchev¹³⁶, P.M. Gravila^{27f},
 F.G. Gravili^{67a,67b}, C. Gray⁵⁷, H.M. Gray¹⁸, C. Grefe²⁴, I.M. Gregor⁴⁶, P. Grenier¹⁵²,
 K. Grevtsov⁴⁶, C. Grieco¹⁴, N.A. Grieser¹²⁷, A.A. Grillo¹⁴⁴, K. Grimm^{31,l}, S. Grinstein^{14,w},
 J.-F. Grivaz⁶⁴, S. Groh⁹⁹, E. Gross¹⁷⁸, J. Grosse-Knetter⁵³, Z.J. Grout⁹⁴, C. Grud¹⁰⁵,
 A. Grummer¹¹⁷, J.C. Grundy¹³³, L. Guan¹⁰⁵, W. Guan¹⁷⁹, C. Gubbels¹⁷³, J. Guenther³⁶,
 J.G.R. Guerrero Rojas¹⁷², F. Guescini¹¹⁴, D. Guest^{76,19}, R. Gugel⁹⁹, A. Guida⁴⁶, T. Guillemín⁵,
 S. Guindon³⁶, J. Guo^{60c}, Z. Guo¹⁰¹, R. Gupta⁴⁶, S. Gurbuz^{12c}, G. Gustavino¹²⁷, M. Guth⁵²,
 P. Gutierrez¹²⁷, L.F. Gutierrez Zagazeta¹³⁵, C. Gutsche⁹⁴, C. Guyot¹⁴³, C. Gwenlan¹³³,
 C.B. Gwilliam⁹⁰, E.S. Haaland¹³², A. Haas¹²⁴, C. Haber¹⁸, H.K. Hadavand⁸, A. Hadel⁹⁹,
 M. Haleem¹⁷⁵, J. Haley¹²⁸, J.J. Hall¹⁴⁸, G. Halladjian¹⁰⁶, G.D. Hallewell¹⁰¹, K. Hamano¹⁷⁴,
 H. Hamdaoui^{35f}, M. Hamer²⁴, G.N. Hamity⁵⁰, K. Han^{60a}, L. Han^{15c}, L. Han^{60a}, S. Han¹⁸,
 Y.F. Han¹⁶⁵, K. Hanagaki^{81,u}, M. Hance¹⁴⁴, M.D. Hank³⁷, R. Hankache¹⁰⁰, E. Hansen⁹⁶,
 J.B. Hansen⁴⁰, J.D. Hansen⁴⁰, M.C. Hansen²⁴, P.H. Hansen⁴⁰, E.C. Hanson¹⁰⁰, K. Hara¹⁶⁷,
 T. Harenberg¹⁸⁰, S. Harkusha¹⁰⁷, P.F. Harrison¹⁷⁶, N.M. Hartman¹⁵², N.M. Hartmann¹¹³,
 Y. Hasegawa¹⁴⁹, A. Hasib⁵⁰, S. Hassani¹⁴³, S. Haug²⁰, R. Hauser¹⁰⁶, M. Havranek¹⁴⁰,
 C.M. Hawkes²¹, R.J. Hawkings³⁶, S. Hayashida¹¹⁶, D. Hayden¹⁰⁶, C. Hayes¹⁰⁵, R.L. Hayes¹⁷³,
 C.P. Hays¹³³, J.M. Hays⁹², H.S. Hayward⁹⁰, S.J. Haywood¹⁴², F. He^{60a}, Y. He¹⁶³, M.P. Heath⁵⁰,
 V. Hedberg⁹⁶, A.L. Heggelund¹³², N.D. Hehir⁹², C. Heidegger⁵², K.K. Heidegger⁵²,
 W.D. Heidorn⁷⁸, J. Heilman³⁴, S. Heim⁴⁶, T. Heim¹⁸, B. Heinemann^{46,ai}, J.G. Heinlein¹³⁵,
 J.J. Heinrich¹³⁰, L. Heinrich³⁶, J. Hejbal¹³⁹, L. Helary⁴⁶, A. Held¹²⁴, S. Hellesund¹³²,
 C.M. Helling¹⁴⁴, S. Hellman^{45a,45b}, C. Helsens³⁶, R.C.W. Henderson⁸⁹, L. Henkelmann³²,
 A.M. Henriques Correia³⁶, H. Herde¹⁵², Y. Hernández Jiménez^{33e}, H. Herr⁹⁹, M.G. Herrmann¹¹³,
 T. Herrmann⁴⁸, G. Herten⁵², R. Hertenberger¹¹³, L. Hervas³⁶, N.P. Hessey^{166a}, H. Hibi⁸²,
 S. Higashino⁸¹, E. Higón-Rodríguez¹⁷², K. Hildebrand³⁷, J.C. Hill³², K.K. Hill²⁹, K.H. Hiller⁴⁶,
 S.J. Hillier²¹, M. Hils⁴⁸, I. Hinchliffe¹⁸, F. Hinterkeuser²⁴, M. Hirose¹³¹, S. Hirose¹⁶⁷,
 D. Hirschbuehl¹⁸⁰, B. Hiti⁹¹, O. Hladik¹³⁹, J. Hobbs¹⁵⁴, R. Hobincu^{27e}, N. Hod¹⁷⁸,

M.C. Hodgkinson¹⁴⁸, A. Hoecker³⁶, D. Hohn⁵², D. Hohov⁶⁴, T. Holm²⁴, T.R. Holmes³⁷,
M. Holzbock¹¹⁴, L.B.A.H. Hommels³², T.M. Hong¹³⁷, J.C. Honig⁵², A. Hönle¹¹⁴,
B.H. Hoerberman¹⁷¹, W.H. Hopkins⁶, Y. Horii¹¹⁶, P. Horn⁴⁸, L.A. Horyn³⁷, S. Hou¹⁵⁷,
J. Howarth⁵⁷, J. Hoya⁸⁸, M. Hrabovsky¹²⁹, J. Hrivnac⁶⁴, A. Hrynevich¹⁰⁸, T. Hryn'ova⁵,
P.J. Hsu⁶³, S.-C. Hsu¹⁴⁷, Q. Hu³⁹, S. Hu^{60c}, Y.F. Hu^{15a,15d,am}, D.P. Huang⁹⁴, X. Huang^{15c},
Y. Huang^{60a}, Y. Huang^{15a}, Z. Hubacek¹⁴⁰, F. Hubaut¹⁰¹, M. Huebner²⁴, F. Huegging²⁴,
T.B. Huffman¹³³, M. Huhtinen³⁶, R. Hulsken⁵⁸, R.F.H. Hunter³⁴, N. Huseynov^{79,ab}, J. Huston¹⁰⁶,
J. Huth⁵⁹, R. Hyneman¹⁵², S. Hyrych^{28a}, G. Iacobucci⁵⁴, G. Iakovidis²⁹, I. Ibragimov¹⁵⁰,
L. Iconomidou-Fayard⁶⁴, P. Iengo³⁶, R. Ignazzi⁴⁰, R. Iguchi¹⁶², T. Iizawa⁵⁴, Y. Ikegami⁸¹,
N. Ilic^{165,165}, H. Imam^{35a}, G. Introzzi^{70a,70b}, M. Iodice^{74a}, K. Iordanidou^{166a}, V. Ippolito^{72a,72b},
M.F. Isacson¹⁷⁰, M. Ishino¹⁶², W. Islam¹²⁸, C. Issever^{19,46}, S. Istin^{12c}, J.M. Iturbe Ponce^{62a},
R. Iuppa^{75a,75b}, A. Ivina¹⁷⁸, J.M. Izen⁴³, V. Izzo^{69a}, P. Jacka¹³⁹, P. Jackson¹, R.M. Jacobs⁴⁶,
B.P. Jaeger¹⁵¹, G. Jäkel¹⁸⁰, K.B. Jakobi⁹⁹, K. Jakobs⁵², T. Jakoubek¹⁷⁸, J. Jamieson⁵⁷,
K.W. Janas^{83a}, R. Jansky⁵⁴, P.A. Janus^{83a}, G. Jarlskog⁹⁶, A.E. Jaspán⁹⁰, N. Javadov^{79,ab},
T. Javůrek³⁶, M. Javurkova¹⁰², F. Jeanneau¹⁴³, L. Jeanty¹³⁰, J. Jejelava^{158a}, P. Jenni^{52,d},
S. Jézéquel⁵, J. Jia¹⁵⁴, Z. Jia^{15c}, Y. Jiang^{60a}, S. Jiggins⁵², F.A. Jimenez Morales³⁸,
J. Jimenez Pena¹¹⁴, S. Jin^{15c}, A. Jinaru^{27b}, O. Jinnouchi¹⁶³, H. Jivan^{33e}, P. Johansson¹⁴⁸,
K.A. Johns⁷, C.A. Johnson⁶⁵, E. Jones¹⁷⁶, R.W.L. Jones⁸⁹, S.D. Jones¹⁵⁵, T.J. Jones⁹⁰,
J. Jovicevic³⁶, X. Ju¹⁸, J.J. Junggeburth¹¹⁴, A. Juste Rozas^{14,w}, A. Kaczmarska⁸⁴,
M. Kado^{72a,72b}, H. Kagan¹²⁶, M. Kagan¹⁵², A. Kahn³⁹, C. Kahra⁹⁹, T. Kaji¹⁷⁷, E. Kajomovitz¹⁵⁹,
C.W. Kalderon²⁹, A. Kaluza⁹⁹, A. Kamenshchikov¹²², M. Kaneda¹⁶², N.J. Kang¹⁴⁴, S. Kang⁷⁸,
Y. Kano¹¹⁶, J. Kanzaki⁸¹, D. Kar^{33e}, K. Karava¹³³, M.J. Kareem^{166b}, I. Karkanas¹⁶¹,
S.N. Karpov⁷⁹, Z.M. Karpova⁷⁹, V. Kartvelishvili⁸⁹, A.N. Karyukhin¹²², E. Kasimi¹⁶¹,
A. Kastanas^{45a,45b}, C. Kato^{60d}, J. Katzy⁴⁶, K. Kawade¹⁴⁹, K. Kawagoe⁸⁷, T. Kawaguchi¹¹⁶,
T. Kawamoto¹⁴³, G. Kawamura⁵³, E.F. Kay¹⁷⁴, F.I. Kaya¹⁶⁸, S. Kazakos¹⁴, V.F. Kazanin^{121b,121a},
J.M. Keaveney^{33a}, R. Keeler¹⁷⁴, J.S. Keller³⁴, D. Kelsey¹⁵⁵, J.J. Kempster²¹, J. Kendrick²¹,
K.E. Kennedy³⁹, O. Kepka¹³⁹, S. Kersten¹⁸⁰, B.P. Kerševan⁹¹, S. Ketabchi Haghighat¹⁶⁵,
F. Khalil-Zada¹³, M. Khandoga¹⁴³, A. Khanov¹²⁸, A.G. Kharlamov^{121b,121a},
T. Kharlamova^{121b,121a}, E.E. Khoda¹⁷³, T.J. Khoo^{76,19}, G. Khoriauli¹⁷⁵, E. Khramov⁷⁹,
J. Khubua^{158b}, S. Kido⁸², M. Kiehn³⁶, A. Kilgallon¹³⁰, E. Kim¹⁶³, Y.K. Kim³⁷, N. Kimura⁹⁴,
A. Kirchhoff⁵³, D. Kirchmeier⁴⁸, J. Kirk¹⁴², A.E. Kiryunin¹¹⁴, T. Kishimoto¹⁶², D.P. Kisluk¹⁶⁵,
V. Kitali⁴⁶, C. Kitsaki¹⁰, O. Kivernyk²⁴, T. Klapdor-Kleingrothaus⁵², M. Klassen^{61a}, C. Klein³⁴,
L. Klein¹⁷⁵, M.H. Klein¹⁰⁵, M. Klein⁹⁰, U. Klein⁹⁰, P. Klimek³⁶, A. Klimentov²⁹, F. Klimpel³⁶,
T. Klingl²⁴, T. Klioutchnikova³⁶, F.F. Klitzner¹¹³, P. Kluit¹¹⁹, S. Kluth¹¹⁴, E. Kneringer⁷⁶,
E.B.F.G. Knoop¹⁰¹, A. Knue⁵², D. Kobayashi⁸⁷, M. Kobel⁴⁸, M. Kocian¹⁵², T. Kodama¹⁶²,
P. Kodys¹⁴¹, D.M. Koehn¹⁵⁵, P.T. Koenig²⁴, T. Koffas³⁴, N.M. Köhler³⁶, M. Kolb¹⁴³,
I. Koletsou⁵, T. Komarek¹²⁹, K. Köneke⁵², A.X.Y. Kong¹, T. Kono¹²⁵, V. Konstantinides⁹⁴,
N. Konstantinidis⁹⁴, B. Konya⁹⁶, R. Kopeliansky⁶⁵, S. Koperny^{83a}, K. Korcyl⁸⁴, K. Kordas¹⁶¹,
G. Koren¹⁶⁰, A. Korn⁹⁴, I. Korolkov¹⁴, E.V. Korolkova¹⁴⁸, N. Korotkova¹¹², O. Kortner¹¹⁴,
S. Kortner¹¹⁴, V.V. Kostyukhin^{148,164}, A. Kotschechagia⁶⁴, A. Kotwal⁴⁹, A. Koulouris¹⁰,
A. Kourkoumeli-Charalampidi^{70a,70b}, C. Kourkoumelis⁹, E. Kourlitis⁶, R. Kowalewski¹⁷⁴,
W. Kozanecki¹⁴³, A.S. Kozhin¹²², V.A. Kramarenko¹¹², G. Kramberger⁹¹, D. Krasnopevtsev^{60a},
M.W. Krasny¹³⁴, A. Krasznahorkay³⁶, J.A. Kremer⁹⁹, J. Kretzschmar⁹⁰, K. Kreul¹⁹, P. Krieger¹⁶⁵,
F. Krieter¹¹³, S. Krishnamurthy¹⁰², A. Krishnan^{61b}, M. Krivos¹⁴¹, K. Krizka¹⁸, K. Kroeninger⁴⁷,
H. Kroha¹¹⁴, J. Kroll¹³⁹, J. Kroll¹³⁵, K.S. Krowpman¹⁰⁶, U. Kruchonak⁷⁹, H. Krüger²⁴,
N. Krumnack⁷⁸, M.C. Kruse⁴⁹, J.A. Krzysiak⁸⁴, A. Kubota¹⁶³, O. Kuchinskaia¹⁶⁴, S. Kудay^{4b},
D. Kuechler⁴⁶, J.T. Kuechler⁴⁶, S. Kuehn³⁶, T. Kuhl⁴⁶, V. Kukhtin⁷⁹, Y. Kulchitsky^{107,ae},
S. Kuleshov^{145b}, Y.P. Kulinich¹⁷¹, M. Kumar^{33e}, M. Kuna⁵⁸, A. Kupco¹³⁹, T. Kupfer⁴⁷,

O. Kuprash⁵², H. Kurashige⁸², L.L. Kurchaninov^{166a}, Y.A. Kurochkin¹⁰⁷, A. Kurova¹¹¹,
 M.G. Kurth^{15a,15d}, E.S. Kuwertz³⁶, M. Kuze¹⁶³, A.K. Kvam¹⁴⁷, J. Kvita¹²⁹, T. Kwan¹⁰³,
 C. Lacasta¹⁷², F. Lacava^{72a,72b}, D.P.J. Lack¹⁰⁰, H. Lacker¹⁹, D. Lacour¹³⁴, E. Ladygin⁷⁹,
 R. Lafaye⁵, B. Laforge¹³⁴, T. Lagouri^{145c}, S. Lai⁵³, I.K. Lakomic^{83a}, J.E. Lambert¹²⁷,
 S. Lammers⁶⁵, W. Lampl⁷, C. Lampoudis¹⁶¹, E. Lançon²⁹, U. Landgraf⁵², M.P.J. Landon⁹²,
 V.S. Lang⁵², J.C. Lange⁵³, R.J. Langenberg¹⁰², A.J. Lankford¹⁶⁹, F. Lanni²⁹, K. Lantzsich²⁴,
 A. Lanza^{70a}, A. Lapertosa^{55b,55a}, J.F. Laporte¹⁴³, T. Lari^{68a}, F. Lasagni Manghi^{23b,23a},
 M. Lassnig³⁶, V. Latonova¹³⁹, T.S. Lau^{62a}, A. Laudrain⁹⁹, A. Laurier³⁴, M. Lavorgna^{69a,69b},
 S.D. Lawlor⁹³, M. Lazzaroni^{68a,68b}, B. Le¹⁰⁰, E. Le Guirriec¹⁰¹, A. Lebedev⁷⁸, M. LeBlanc⁷,
 T. LeCompte⁶, F. Ledroit-Guillon⁵⁸, A.C.A. Lee⁹⁴, C.A. Lee²⁹, G.R. Lee¹⁷, L. Lee⁵⁹, S.C. Lee¹⁵⁷,
 S. Lee⁷⁸, B. Lefebvre^{166a}, H.P. Lefebvre⁹³, M. Lefebvre¹⁷⁴, C. Leggett¹⁸, K. Lehmann¹⁵¹,
 N. Lehmann²⁰, G. Lehmann Miotto³⁶, W.A. Leight⁴⁶, A. Leisos^{161,v}, M.A.L. Leite^{80c},
 C.E. Leitgeb¹¹³, R. Leitner¹⁴¹, K.J.C. Leney⁴², T. Lenz²⁴, S. Leone^{71a}, C. Leonidopoulos⁵⁰,
 A. Leopold¹³⁴, C. Leroy¹⁰⁹, R. Les¹⁰⁶, C.G. Lester³², M. Levchenko¹³⁶, J. Levêque⁵, D. Levin¹⁰⁵,
 L.J. Levinson¹⁷⁸, D.J. Lewis²¹, B. Li^{15b}, B. Li¹⁰⁵, C-Q. Li^{60c,60d}, F. Li^{60c}, H. Li^{60a}, H. Li^{60b},
 J. Li^{60c}, K. Li¹⁴⁷, L. Li^{60c}, M. Li^{15a,15d}, Q.Y. Li^{60a}, S. Li^{60d,60c,b}, X. Li⁴⁶, Y. Li⁴⁶, Z. Li^{60b},
 Z. Li¹³³, Z. Li¹⁰³, Z. Li⁹⁰, Z. Liang^{15a}, M. Liberatore⁴⁶, B. Liberti^{73a}, K. Lie^{62c}, S. Lim²⁹,
 C.Y. Lin³², K. Lin¹⁰⁶, R.A. Linck⁶⁵, R.E. Lindley⁷, J.H. Lindon²¹, A. Linss⁴⁶, A.L. Lioni⁵⁴,
 E. Lipeles¹³⁵, A. Lipniacka¹⁷, T.M. Liss^{171,aj}, A. Lister¹⁷³, J.D. Little⁸, B. Liu⁷⁸, B.X. Liu¹⁵¹,
 J.B. Liu^{60a}, J.K.K. Liu³⁷, K. Liu^{60d,60c}, M. Liu^{60a}, M.Y. Liu^{60a}, P. Liu^{15a}, X. Liu^{60a}, Y. Liu⁴⁶,
 Y. Liu^{15a,15d}, Y.L. Liu¹⁰⁵, Y.W. Liu^{60a}, M. Livan^{70a,70b}, A. Lleres⁵⁸, J. Llorente Merino¹⁵¹,
 S.L. Lloyd⁹², E.M. Lobodzinska⁴⁶, P. Loch⁷, S. Loffredo^{73a,73b}, T. Lohse¹⁹, K. Lohwasser¹⁴⁸,
 M. Lokajicek¹³⁹, J.D. Long¹⁷¹, R.E. Long⁸⁹, I. Longarini^{72a,72b}, L. Longo³⁶, R. Longo¹⁷¹,
 I. Lopez Paz¹⁰⁰, A. Lopez Solis¹⁴⁸, J. Lorenz¹¹³, N. Lorenzo Martinez⁵, A.M. Lory¹¹³, A. Lösle⁵²,
 X. Lou^{45a,45b}, X. Lou^{15a}, A. Lounis⁶⁴, J. Love⁶, P.A. Love⁸⁹, J.J. Lozano Bahilo¹⁷², M. Lu^{60a},
 S. Lu¹³⁵, Y.J. Lu⁶³, H.J. Lubatti¹⁴⁷, C. Luci^{72a,72b}, F.L. Lucio Alves^{15c}, A. Lucotte⁵⁸,
 F. Luehring⁶⁵, I. Luise¹⁵⁴, L. Luminari^{72a}, B. Lund-Jensen¹⁵³, N.A. Luongo¹³⁰, M.S. Lutz¹⁶⁰,
 D. Lynn²⁹, H. Lyons⁹⁰, R. Lysak¹³⁹, E. Lytken⁹⁶, F. Lyu^{15a}, V. Lyubushkin⁷⁹, T. Lyubushkina⁷⁹,
 H. Ma²⁹, L.L. Ma^{60b}, Y. Ma⁹⁴, D.M. Mac Donnell¹⁷⁴, G. Maccarrone⁵¹, C.M. Macdonald¹⁴⁸,
 J.C. MacDonald¹⁴⁸, J. Machado Miguens¹³⁵, R. Madar³⁸, W.F. Mader⁴⁸,
 M. Madugoda Ralalage Don¹²⁸, N. Madysa⁴⁸, J. Maeda⁸², T. Maeno²⁹, M. Maerker⁴⁸,
 V. Magerl⁵², J. Magro^{66a,66c,r}, D.J. Mahon³⁹, C. Maidantchik^{80b}, A. Maio^{138a,138b,138d}, K. Maj^{83a},
 O. Majersky^{28a}, S. Majewski¹³⁰, N. Makovec⁶⁴, B. Malaescu¹³⁴, Pa. Malecki⁸⁴, V.P. Maleev¹³⁶,
 F. Malek⁵⁸, D. Malito^{41b,41a}, U. Mallik⁷⁷, C. Malone³², S. Maltezos¹⁰, S. Malyukov⁷⁹,
 J. Mamuzic¹⁷², G. Mancini⁵¹, J.P. Mandalia⁹², I. Mandić⁹¹, L. Manhaes de Andrade Filho^{80a},
 I.M. Maniatis¹⁶¹, J. Manjarres Ramos⁴⁸, K.H. Mankinen⁹⁶, A. Mann¹¹³, A. Manousos⁷⁶,
 B. Mansoulie¹⁴³, I. Manthos¹⁶¹, S. Manzoni¹¹⁹, A. Marantis¹⁶¹, L. Marchese¹³³, G. Marchiori¹³⁴,
 M. Marcisovsky¹³⁹, L. Marcoccia^{73a,73b}, C. Marcon⁹⁶, M. Marjanovic¹²⁷, Z. Marshall¹⁸,
 M.U.F. Martensson¹⁷⁰, S. Marti-Garcia¹⁷², T.A. Martin¹⁷⁶, V.J. Martin⁵⁰,
 B. Martin dit Latour¹⁷, L. Martinelli^{74a,74b}, M. Martinez^{14,w}, P. Martinez Agullo¹⁷²,
 V.I. Martinez Outschoorn¹⁰², S. Martin-Haugh¹⁴², V.S. Martoiu^{27b}, A.C. Martyniuk⁹⁴,
 A. Marzin³⁶, S.R. Maschek¹¹⁴, L. Masetti⁹⁹, T. Mashimo¹⁶², R. Mashinistov¹¹⁰, J. Masik¹⁰⁰,
 A.L. Maslennikov^{121b,121a}, L. Massa^{23b,23a}, P. Massarotti^{69a,69b}, P. Mastrandrea^{71a,71b},
 A. Mastroberardino^{41b,41a}, T. Masubuchi¹⁶², D. Matakias²⁹, T. Mathisen¹⁷⁰, A. Matić¹¹³,
 N. Matsuzawa¹⁶², J. Maurer^{27b}, B. Maček⁹¹, D.A. Maximov^{121b,121a}, R. Mazini¹⁵⁷, I. Maznas¹⁶¹,
 S.M. Mazza¹⁴⁴, C. Mc Ginn²⁹, J.P. Mc Gowan¹⁰³, S.P. Mc Kee¹⁰⁵, T.G. McCarthy¹¹⁴,
 W.P. McCormack¹⁸, E.F. McDonald¹⁰⁴, A.E. McDougall¹¹⁹, J.A. Mcfayden¹⁸, G. Mchedlidze^{158b},
 M.A. McKay⁴², K.D. McLean¹⁷⁴, S.J. McMahon¹⁴², P.C. McNamara¹⁰⁴, C.J. McNicol¹⁷⁶,

R.A. McPherson^{174,aa}, J.E. Mdhli^{33e}, Z.A. Meadows¹⁰², S. Meehan³⁶, T. Megy³⁸,
S. Mehlhase¹¹³, A. Mehta⁹⁰, B. Meirose⁴³, D. Melini¹⁵⁹, B.R. Mellado Garcia^{33e}, F. Meloni⁴⁶,
A. Melzer²⁴, E.D. Mendes Gouveia^{138a,138e}, A.M. Mendes Jacques Da Costa²¹, H.Y. Meng¹⁶⁵,
L. Meng³⁶, S. Menke¹¹⁴, E. Meoni^{41b,41a}, S. Mergelmeyer¹⁹, S.A.M. Merkt¹³⁷, C. Merlassino¹³³,
P. Mermod⁵⁴, L. Merola^{69a,69b}, C. Meroni^{68a}, G. Merz¹⁰⁵, O. Meshkov^{112,110}, J.K.R. Meshreki¹⁵⁰,
J. Metcalfe⁶, A.S. Mete⁶, C. Meyer⁶⁵, J.-P. Meyer¹⁴³, M. Michetti¹⁹, R.P. Middleton¹⁴²,
L. Mijović⁵⁰, G. Mikenberg¹⁷⁸, M. Mikestikova¹³⁹, M. Mikuz⁹¹, H. Mildner¹⁴⁸, A. Milic¹⁶⁵,
C.D. Milke⁴², D.W. Miller³⁷, L.S. Miller³⁴, A. Milov¹⁷⁸, D.A. Milstead^{45a,45b}, A.A. Minaenko¹²²,
I.A. Minashvili^{158b}, L. Mince⁵⁷, A.I. Mincer¹²⁴, B. Mindur^{83a}, M. Mineev⁷⁹, Y. Minegishi¹⁶²,
Y. Mino⁸⁵, L.M. Mir¹⁴, M. Mironova¹³³, T. Mitani¹⁷⁷, J. Mitrevski¹¹³, V.A. Mitsou¹⁷²,
M. Mittal^{60c}, O. Miu¹⁶⁵, A. Miucci²⁰, P.S. Miyagawa⁹², A. Mizukami⁸¹, J.U. Mjörnmark⁹⁶,
T. Mkrtchyan^{61a}, M. Mlynarikova¹²⁰, T. Moa^{45a,45b}, S. Mobius⁵³, K. Mochizuki¹⁰⁹, P. Moder⁴⁶,
P. Mogg¹¹³, S. Mohapatra³⁹, G. Mokgatitswane^{33e}, B. Mondal¹⁵⁰, S. Mondal¹⁴⁰, K. Mönig⁴⁶,
E. Monnier¹⁰¹, A. Montalbano¹⁵¹, J. Montejo Berlingen³⁶, M. Montella⁹⁴, F. Monticelli⁸⁸,
N. Morange⁶⁴, A.L. Moreira De Carvalho^{138a}, M. Moreno Llácer¹⁷², C. Moreno Martinez¹⁴,
P. Morettini^{55b}, M. Morgenstern¹⁵⁹, S. Morgenstern¹⁷⁶, D. Mori¹⁵¹, M. Morii⁵⁹, M. Morinaga¹⁷⁷,
V. Morisbak¹³², A.K. Morley³⁶, G. Mornacchi³⁶, A.P. Morris⁹⁴, L. Morvaj³⁶, P. Moschovakos³⁶,
B. Moser¹¹⁹, M. Mosidze^{158b}, T. Moskalets¹⁴³, P. Moskvitina¹¹⁸, J. Moss^{31,n}, E.J.W. Moyse¹⁰²,
S. Muanza¹⁰¹, J. Mueller¹³⁷, D. Muenstermann⁸⁹, G.A. Mullier⁹⁶, J.J. Mullin¹³⁵,
D.P. Mungo^{68a,68b}, J.L. Munoz Martinez¹⁴, F.J. Munoz Sanchez¹⁰⁰, P. Murin^{28b},
W.J. Murray^{176,142}, A. Murrone^{68a,68b}, J.M. Muse¹²⁷, M. Muškinja¹⁸, C. Mwewa^{33a},
A.G. Myagkov^{122,af}, A.A. Myers¹³⁷, G. Myers⁶⁵, J. Myers¹³⁰, M. Myska¹⁴⁰, B.P. Nachman¹⁸,
O. Nackenhorst⁴⁷, A. Nag Nag⁴⁸, K. Nagai¹³³, K. Nagano⁸¹, J.L. Nagle²⁹, E. Nagy¹⁰¹,
A.M. Nairz³⁶, Y. Nakahama¹¹⁶, K. Nakamura⁸¹, H. Nanjo¹³¹, F. Napolitano^{61a},
R.F. Naranjo Garcia⁴⁶, R. Narayan⁴², I. Naryshkin¹³⁶, M. Naseri³⁴, T. Naumann⁴⁶,
G. Navarro^{22a}, J. Navarro-Gonzalez¹⁷², P.Y. Nechaeva¹¹⁰, F. Nechansky⁴⁶, T.J. Neep²¹,
A. Negri^{70a,70b}, M. Negrini^{23b}, C. Nellist¹¹⁸, C. Nelson¹⁰³, M.E. Nelson^{45a,45b}, S. Nemecek¹³⁹,
M. Nessi^{36,f}, M.S. Neubauer¹⁷¹, F. Neuhaus⁹⁹, M. Neumann¹⁸⁰, R. Newhouse¹⁷³, P.R. Newman²¹,
C.W. Ng¹³⁷, Y.S. Ng¹⁹, Y.W.Y. Ng¹⁶⁹, B. Ngai^{35f}, H.D.N. Nguyen¹⁰¹, T. Nguyen Manh¹⁰⁹,
E. Nibigira³⁸, R.B. Nickerson¹³³, R. Nicolaidou¹⁴³, D.S. Nielsen⁴⁰, J. Nielsen¹⁴⁴, M. Niemeyer⁵³,
N. Nikiforou¹¹, V. Nikolaenko^{122,af}, I. Nikolic-Audit¹³⁴, K. Nikolopoulos²¹, P. Nilsson²⁹,
H.R. Nindhito⁵⁴, A. Nisati^{72a}, N. Nishu^{60c}, R. Nisius¹¹⁴, I. Nitsche⁴⁷, T. Nitta¹⁷⁷, T. Nobe¹⁶²,
D.L. Noel³², Y. Noguchi⁸⁵, I. Nomidis¹³⁴, M.A. Nomura²⁹, M. Nordberg³⁶, R.R.B. Norisam⁹⁴,
J. Novak⁹¹, T. Novak⁹¹, O. Novgorodova⁴⁸, R. Novotny¹¹⁷, L. Nozka¹²⁹, K. Ntekas¹⁶⁹, E. Nurse⁹⁴,
F.G. Oakham^{34,ak}, J. Ocariz¹³⁴, A. Ochi⁸², I. Ochoa^{138a}, J.P. Ochoa-Ricoux^{145a}, K. O'Connor²⁶,
S. Oda⁸⁷, S. Odaka⁸¹, S. Oerdek⁵³, A. Ogrodnik^{83a}, A. Oh¹⁰⁰, C.C. Ohm¹⁵³, H. Oide¹⁶³,
R. Oishi¹⁶², M.L. Ojeda¹⁶⁵, Y. Okazaki⁸⁵, M.W. O'Keefe⁹⁰, Y. Okumura¹⁶², A. Olariu^{27b},
L.F. Oleiro Seabra^{138a}, S.A. Olivares Pino^{145a}, D. Oliveira Damazio²⁹, J.L. Oliver¹,
M.J.R. Olsson¹⁶⁹, A. Olszewski⁸⁴, J. Olszowska⁸⁴, Ö.O. Öncel²⁴, D.C. O'Neil¹⁵¹, A.P. O'Neill¹³³,
A. Onofre^{138a,138e}, P.U.E. Onyisi¹¹, H. Oppen¹³², R.G. Oreamuno Madriz¹²⁰, M.J. Oreglia³⁷,
G.E. Orellana⁸⁸, D. Orestano^{74a,74b}, N. Orlando¹⁴, R.S. Orr¹⁶⁵, V. O'Shea⁵⁷, R. Ospanov^{60a},
G. Otero y Garzon³⁰, H. Otono⁸⁷, P.S. Ott^{61a}, G.J. Ottino¹⁸, M. Ouchrif^{35e}, J. Ouellette²⁹,
F. Ould-Saada¹³², A. Ouraou^{143,*}, Q. Ouyang^{15a}, M. Owen⁵⁷, R.E. Owen¹⁴², V.E. Ozcan^{12c},
N. Ozturk⁸, J. Pacalt¹²⁹, H.A. Pacey³², K. Pachal⁴⁹, A. Pacheco Pages¹⁴, C. Padilla Aranda¹⁴,
S. Pagan Griso¹⁸, G. Palacino⁶⁵, S. Palazzo⁵⁰, S. Palestini³⁶, M. Palka^{83b}, P. Palni^{83a},
D.K. Panchal¹¹, C.E. Pandini⁵⁴, J.G. Panduro Vazquez⁹³, P. Pani⁴⁶, G. Panizzo^{66a,66c},
L. Paolozzi⁵⁴, C. Papadatos¹⁰⁹, K. Papageorgiou^{9,h}, S. Parajuli⁴², A. Paramonov⁶,
C. Paraskevopoulos¹⁰, D. Paredes Hernandez^{62b}, S.R. Paredes Saenz¹³³, B. Parida¹⁷⁸,

T.H. Park¹⁶⁵, A.J. Parker³¹, M.A. Parker³², F. Parodi^{55b,55a}, E.W. Parrish¹²⁰, J.A. Parsons³⁹, U. Parzefall⁵², L. Pascual Dominguez¹³⁴, V.R. Pascuzzi¹⁸, J.M.P. Pasner¹⁴⁴, F. Pasquali¹¹⁹, E. Pasqualucci^{72a}, S. Passaggio^{55b}, F. Pastore⁹³, P. Pasuwan^{45a,45b}, J.R. Pater¹⁰⁰, A. Pathak^{179,j}, J. Patton⁹⁰, T. Pauly³⁶, J. Pearkes¹⁵², M. Pedersen¹³², L. Pedraza Diaz¹¹⁸, R. Pedro^{138a}, T. Peiffer⁵³, S.V. Peleganchuk^{121b,121a}, O. Penc¹³⁹, C. Peng^{62b}, H. Peng^{60a}, B.S. Peralva^{80a}, M.M. Perego⁶⁴, A.P. Pereira Peixoto^{138a}, L. Pereira Sanchez^{45a,45b}, D.V. Perepelitsa²⁹, E. Perez Codina^{166a}, L. Perini^{68a,68b}, H. Pernegger³⁶, S. Perrella³⁶, A. Perrevoort¹¹⁹, K. Peters⁴⁶, R.F.Y. Peters¹⁰⁰, B.A. Petersen³⁶, T.C. Petersen⁴⁰, E. Petit¹⁰¹, V. Petousis¹⁴⁰, C. Petridou¹⁶¹, P. Petroff⁶⁴, F. Petrucci^{74a,74b}, M. Pettee¹⁸¹, N.E. Pettersson¹⁰², K. Petukhova¹⁴¹, A. Peyaud¹⁴³, R. Pezoa^{145d}, L. Pezzotti^{70a,70b}, G. Pezzullo¹⁸¹, T. Pham¹⁰⁴, P.W. Phillips¹⁴², M.W. Phipps¹⁷¹, G. Piacquadio¹⁵⁴, E. Pianori¹⁸, A. Picazio¹⁰², R.H. Pickles¹⁰⁰, R. Piegai³⁰, D. Pietreanu^{27b}, J.E. Pilcher³⁷, A.D. Pilkington¹⁰⁰, M. Pinamonti^{66a,66c}, J.L. Pinfold³, C. Pitman Donaldson⁹⁴, L. Pizzimento^{73a,73b}, A. Pizzini¹¹⁹, M.-A. Pleier²⁹, V. Plesanovs⁵², V. Pleskot¹⁴¹, E. Plotnikova⁷⁹, P. Podberezko^{121b,121a}, R. Poettgen⁹⁶, R. Poggi⁵⁴, L. Poggioli¹³⁴, I. Pogrebnyak¹⁰⁶, D. Pohl²⁴, I. Pokharel⁵³, G. Polesello^{70a}, A. Poley^{151,166a}, A. Policicchio^{72a,72b}, R. Polifka¹⁴¹, A. Polini^{23b}, C.S. Pollard⁴⁶, V. Polychronakos²⁹, D. Ponomarenko¹¹¹, L. Pontecorvo³⁶, S. Popa^{27a}, G.A. Popeneciu^{27d}, L. Portales⁵, D.M. Portillo Quintero⁵⁸, S. Pospisil¹⁴⁰, P. Postolache^{27c}, K. Potamianos¹³³, I.N. Potrap⁷⁹, C.J. Potter³², H. Potti¹¹, T. Poulsen⁹⁶, J. Poveda¹⁷², T.D. Powell¹⁴⁸, G. Pownall⁴⁶, M.E. Pozo Astigarraga³⁶, A. Prades Ibanez¹⁷², P. Pralavorio¹⁰¹, M.M. Prapa⁴⁴, S. Prell⁷⁸, D. Price¹⁰⁰, M. Primavera^{67a}, M.L. Proffitt¹⁴⁷, N. Proklova¹¹¹, K. Prokofiev^{62c}, F. Prokoshin⁷⁹, S. Protopopescu²⁹, J. Proudfoot⁶, M. Przybycien^{83a}, D. Pudza¹³⁶, A. Puri¹⁷¹, P. Puzo⁶⁴, D. Pyatiizbyantseva¹¹¹, J. Qian¹⁰⁵, Y. Qin¹⁰⁰, A. Quadt⁵³, M. Queitsch-Maitland³⁶, G. Rabanal Bolanos⁵⁹, M. Racko^{28a}, F. Ragusa^{68a,68b}, G. Rahal⁹⁷, J.A. Raine⁵⁴, S. Rajagopalan²⁹, A. Ramirez Morales⁹², K. Ran^{15a,15d}, D.F. Rassloff^{61a}, D.M. Rauch⁴⁶, F. Rauscher¹¹³, S. Rave⁹⁹, B. Ravina⁵⁷, I. Ravinovich¹⁷⁸, M. Raymond³⁶, A.L. Read¹³², N.P. Readioff¹⁴⁸, M. Reale^{67a,67b}, D.M. Rebuffi^{70a,70b}, G. Redlinger²⁹, K. Reeves⁴³, D. Reikher¹⁶⁰, A. Reiss⁹⁹, A. Rej¹⁵⁰, C. Rembser³⁶, A. Renardi⁴⁶, M. Renda^{27b}, M.B. Rendel¹¹⁴, A.G. Rennie⁵⁷, S. Resconi^{68a}, E.D. Resseguie¹⁸, S. Rettie⁹⁴, B. Reynolds¹²⁶, E. Reynolds²¹, O.L. Rezanova^{121b,121a}, P. Reznicek¹⁴¹, E. Ricci^{75a,75b}, R. Richter¹¹⁴, S. Richter⁴⁶, E. Richter-Was^{83b}, M. Ridel¹³⁴, P. Rieck¹¹⁴, O. Rifki⁴⁶, M. Rijssenbeek¹⁵⁴, A. Rimoldi^{70a,70b}, M. Rimoldi⁴⁶, L. Rinaldi^{23b}, T.T. Rinn¹⁷¹, G. Ripellino¹⁵³, I. Riu¹⁴, P. Rivadeneira⁴⁶, J.C. Rivera Vergara¹⁷⁴, F. Rizatdinova¹²⁸, E. Rizvi⁹², C. Rizzi³⁶, S.H. Robertson^{103,aa}, M. Robin⁴⁶, D. Robinson³², C.M. Robles Gajardo^{145d}, M. Robles Manzano⁹⁹, A. Robson⁵⁷, A. Rocchi^{73a,73b}, C. Roda^{71a,71b}, S. Rodriguez Bosca¹⁷², A. Rodriguez Rodriguez⁵², A.M. Rodríguez Vera^{166b}, S. Roe³⁶, J. Roggel¹⁸⁰, O. Röhne¹³², R.A. Rojas^{145d}, B. Roland⁵², C.P.A. Roland⁶⁵, J. Roloff²⁹, A. Romaniouk¹¹¹, M. Romano^{23b,23a}, N. Rompotis⁹⁰, M. Ronzani¹²⁴, L. Roos¹³⁴, S. Rosati^{72a}, G. Rosin¹⁰², B.J. Rosser¹³⁵, E. Rossi⁴⁶, E. Rossi^{74a,74b}, E. Rossi^{69a,69b}, L.P. Rossi^{55b}, L. Rossini⁴⁶, R. Rosten¹²⁶, M. Rotaru^{27b}, B. Rottler⁵², D. Rousseau⁶⁴, G. Rovelli^{70a,70b}, A. Roy¹¹, A. Rozanov¹⁰¹, Y. Rozen¹⁵⁹, X. Ruan^{33e}, A.J. Ruby⁹⁰, T.A. Ruggeri¹, F. Rühr⁵², A. Ruiz-Martinez¹⁷², A. Rummler³⁶, Z. Rurikova⁵², N.A. Rusakovich⁷⁹, H.L. Russell¹⁰³, L. Rustige^{38,47}, J.P. Rutherford⁷, E.M. Rüttinger¹⁴⁸, M. Rybar¹⁴¹, G. Rybkin⁶⁴, E.B. Rye¹³², A. Ryzhov¹²², J.A. Sabater Iglesias⁴⁶, P. Sabatini¹⁷², L. Sabetta^{72a,72b}, S. Sacerdoti⁶⁴, H.F.-W. Sadrozinski¹⁴⁴, R. Sadykov⁷⁹, F. Safai Tehrani^{72a}, B. Safarzadeh Samani¹⁵⁵, M. Safdari¹⁵², P. Saha¹²⁰, S. Saha¹⁰³, M. Sahinsoy¹¹⁴, A. Sahu¹⁸⁰, M. Saimpert³⁶, M. Saito¹⁶², T. Saito¹⁶², D. Salamani⁵⁴, G. Salamanna^{74a,74b}, A. Salnikov¹⁵², J. Salt¹⁷², A. Salvador Salas¹⁴, D. Salvatore^{41b,41a}, F. Salvatore¹⁵⁵, A. Salzburger³⁶, D. Sammel⁵², D. Sampsonidis¹⁶¹, D. Sampsonidou^{60d,60c}, J. Sánchez¹⁷², A. Sanchez Pineda^{66a,36,66c}, H. Sandaker¹³², C.O. Sander⁴⁶, I.G. Sanderswood⁸⁹, M. Sandhoff¹⁸⁰, C. Sandoval^{22b},

D.P.C. Sankey¹⁴², M. Sannino^{55b,55a}, Y. Sano¹¹⁶, A. Sansoni⁵¹, C. Santoni³⁸, H. Santos^{138a,138b},
 S.N. Santpur¹⁸, A. Santra¹⁷⁸, K.A. Saoucha¹⁴⁸, A. Sapronov⁷⁹, J.G. Saraiva^{138a,138d}, O. Sasaki⁸¹,
 K. Sato¹⁶⁷, F. Sauerburger⁵², E. Sauvan⁵, P. Savard^{165,ak}, R. Sawada¹⁶², C. Sawyer¹⁴²,
 L. Sawyer⁹⁵, I. Sayago Galvan¹⁷², C. Sbarra^{23b}, A. Sbrizzi^{66a,66c}, T. Scanlon⁹⁴,
 J. Schaarschmidt¹⁴⁷, P. Schacht¹¹⁴, D. Schaefer³⁷, L. Schaefer¹³⁵, U. Schäfer⁹⁹, A.C. Schaffer⁶⁴,
 D. Schaile¹¹³, R.D. Schamberger¹⁵⁴, E. Schanet¹¹³, C. Scharf¹⁹, N. Scharmberg¹⁰⁰,
 V.A. Schegelsky¹³⁶, D. Scheirich¹⁴¹, F. Schenck¹⁹, M. Schernau¹⁶⁹, C. Schiavi^{55b,55a},
 L.K. Schildgen²⁴, Z.M. Schillaci²⁶, E.J. Schioppa^{67a,67b}, M. Schioppa^{41b,41a}, K.E. Schleicher⁵²,
 S. Schlenker³⁶, K.R. Schmidt-Sommerfeld¹¹⁴, K. Schmieden⁹⁹, C. Schmitt⁹⁹, S. Schmitt⁴⁶,
 L. Schoeffel¹⁴³, A. Schoening^{61b}, P.G. Scholer⁵², E. Schopf¹³³, M. Schott⁹⁹,
 J.F.P. Schouwenberg¹¹⁸, J. Schovancova³⁶, S. Schramm⁵⁴, F. Schroeder¹⁸⁰, A. Schulte⁹⁹,
 H-C. Schultz-Coulon^{61a}, M. Schumacher⁵², B.A. Schumm¹⁴⁴, Ph. Schune¹⁴³, A. Schwartzman¹⁵²,
 T.A. Schwarz¹⁰⁵, Ph. Schwemling¹⁴³, R. Schwienhorst¹⁰⁶, A. Sciandra¹⁴⁴, G. Sciolla²⁶, F. Scuri^{71a},
 F. Scutti¹⁰⁴, L.M. Scyboz¹¹⁴, C.D. Sebastiani⁹⁰, K. Sedlaczek⁴⁷, P. Seema¹⁹, S.C. Seidel¹¹⁷,
 A. Seiden¹⁴⁴, B.D. Seidlitz²⁹, T. Seiss³⁷, C. Seitz⁴⁶, J.M. Seixas^{80b}, G. Sekhniaidze^{69a},
 S.J. Sekula⁴², N. Semprini-Cesari^{23b,23a}, S. Sen⁴⁹, C. Serfon²⁹, L. Serin⁶⁴, L. Serkin^{66a,66b},
 M. Sessa^{60a}, H. Severini¹²⁷, S. Sevova¹⁵², F. Sforza^{55b,55a}, A. Sfyrta⁵⁴, E. Shabalina⁵³,
 J.D. Shahinian¹³⁵, N.W. Shaikh^{45a,45b}, D. Shaked Renous¹⁷⁸, L.Y. Shan^{15a}, M. Shapiro¹⁸,
 A. Sharma³⁶, A.S. Sharma¹, P.B. Shatalov¹²³, K. Shaw¹⁵⁵, S.M. Shaw¹⁰⁰, M. Shehade¹⁷⁸,
 Y. Shen¹²⁷, P. Sherwood⁹⁴, L. Shi⁹⁴, C.O. Shimmin¹⁸¹, Y. Shimogama¹⁷⁷, M. Shimojima¹¹⁵,
 J.D. Shinner⁹³, I.P.J. Shipsey¹³³, S. Shirabe¹⁶³, M. Shiyakova^{79,y}, J. Shlomi¹⁷⁸, A. Shmeleva¹¹⁰,
 M.J. Shochet³⁷, J. Shojaii¹⁰⁴, D.R. Shope¹⁵³, S. Shrestha¹²⁶, E.M. Shrif^{33e}, M.J. Shroff¹⁷⁴,
 E. Shulga¹⁷⁸, P. Sicho¹³⁹, A.M. Sickles¹⁷¹, E. Sideras Haddad^{33e}, O. Sidiropoulou³⁶,
 A. Sidoti^{23b,23a}, F. Siegert⁴⁸, Dj. Sijacki¹⁶, M.V. Silva Oliveira³⁶, S.B. Silverstein^{45a}, S. Simion⁶⁴,
 R. Simoniello⁹⁹, C.J. Simpson-allsoy²¹, S. Simsek^{12b}, P. Sinervo¹⁶⁵, V. Sinetckii¹¹², S. Singh¹⁵¹,
 S. Sinha^{33e}, M. Sioli^{23b,23a}, I. Siral¹³⁰, S.Yu. Sivoklokov¹¹², J. Sjölin^{45a,45b}, A. Skal⁵³, E. Skorda⁹⁶,
 P. Skubic¹²⁷, M. Slawinska⁸⁴, K. Sliwa¹⁶⁸, V. Smakhtin¹⁷⁸, B.H. Smart¹⁴², J. Smiesko^{28b},
 N. Smirnov¹¹¹, S.Yu. Smirnov¹¹¹, Y. Smirnov¹¹¹, L.N. Smirnova^{112,s}, O. Smirnova⁹⁶,
 E.A. Smith³⁷, H.A. Smith¹³³, M. Smizanska⁸⁹, K. Smolek¹⁴⁰, A. Smykiewicz⁸⁴, A.A. Snesarev¹¹⁰,
 H.L. Snoek¹¹⁹, I.M. Snyder¹³⁰, S. Snyder²⁹, R. Sobie^{174,aa}, A. Soffer¹⁶⁰, A. Sögaard⁵⁰, F. Sohns⁵³,
 C.A. Solans Sanchez³⁶, E.Yu. Soldatov¹¹¹, U. Soldevila¹⁷², A.A. Solodkov¹²², A. Soloshenko⁷⁹,
 O.V. Solovyanov¹²², V. Solovyev¹³⁶, P. Sommer¹⁴⁸, H. Son¹⁶⁸, A. Sonay¹⁴, W.Y. Song^{166b},
 A. Sopczak¹⁴⁰, A.L. Soppio⁹⁴, F. Sopkova^{28b}, S. Sottocornola^{70a,70b}, R. Soualah^{66a,66c},
 A.M. Soukharev^{121b,121a}, D. South⁴⁶, S. Spagnolo^{67a,67b}, M. Spalla¹¹⁴, M. Spangenberg¹⁷⁶,
 F. Spanò⁹³, D. Sperlich⁵², T.M. Spieker^{61a}, G. Spigo³⁶, M. Spina¹⁵⁵, D.P. Spiteri⁵⁷,
 M. Spousta¹⁴¹, A. Stabile^{68a,68b}, B.L. Stamas¹²⁰, R. Stamen^{61a}, M. Stamenkovic¹¹⁹,
 A. Stampekis²¹, E. Stanecka⁸⁴, B. Stanislaus¹³³, M.M. Stanitzki⁴⁶, M. Stankaityte¹³³, B. Stapf¹¹⁹,
 E.A. Starchenko¹²², G.H. Stark¹⁴⁴, J. Stark⁵⁸, P. Staroba¹³⁹, P. Starovoitov^{61a}, S. Stärz¹⁰³,
 R. Staszewski⁸⁴, G. Stavropoulos⁴⁴, P. Steinberg²⁹, A.L. Steinhebel¹³⁰, B. Stelzer^{151,166a},
 H.J. Stelzer¹³⁷, O. Stelzer-Chilton^{166a}, H. Stenzel⁵⁶, T.J. Stevenson¹⁵⁵, G.A. Stewart³⁶,
 M.C. Stockton³⁶, G. Stoicea^{27b}, M. Stolarski^{138a}, S. Stonjek¹¹⁴, A. Straessner⁴⁸, J. Strandberg¹⁵³,
 S. Strandberg^{45a,45b}, M. Strauss¹²⁷, T. Strebler¹⁰¹, P. Strizenc^{28b}, R. Ströhmer¹⁷⁵,
 D.M. Strom¹³⁰, R. Stroynowski⁴², A. Strubig^{45a,45b}, S.A. Stucci²⁹, B. Stugu¹⁷, J. Stupak¹²⁷,
 N.A. Styles⁴⁶, D. Su¹⁵², W. Su^{60d,147,60c}, X. Su^{60a}, N.B. Suarez¹³⁷, V.V. Sulin¹¹⁰, M.J. Sullivan⁹⁰,
 D.M.S. Sultan⁵⁴, S. Sultansoy^{4c}, T. Sumida⁸⁵, S. Sun¹⁰⁵, X. Sun¹⁰⁰, C.J.E. Suster¹⁵⁶,
 M.R. Sutton¹⁵⁵, M. Svatos¹³⁹, M. Swiatlowski^{166a}, S.P. Swift², T. Swirski¹⁷⁵, A. Sydorenko⁹⁹,
 I. Sykora^{28a}, M. Sykora¹⁴¹, T. Sykora¹⁴¹, D. Ta⁹⁹, K. Tackmann^{46,x}, J. Taenzer¹⁶⁰, A. Taffard¹⁶⁹,
 R. Tafirout^{166a}, E. Tagiev¹²², R.H.M. Taibah¹³⁴, R. Takashima⁸⁶, K. Takeda⁸², T. Takeshita¹⁴⁹,

E.P. Takeva⁵⁰, Y. Takubo⁸¹, M. Talby¹⁰¹, A.A. Talyshev^{121b,121a}, K.C. Tam^{62b}, N.M. Tamir¹⁶⁰,
 J. Tanaka¹⁶², R. Tanaka⁶⁴, S. Tapia Araya¹⁷¹, S. Tapprogge⁹⁹, A. Tarek Abouelfadl Mohamed¹⁰⁶,
 S. Tarem¹⁵⁹, K. Tariq^{60b}, G. Tarna^{27b,e}, G.F. Tartarelli^{68a}, P. Tas¹⁴¹, M. Tasevsky¹³⁹,
 E. Tassi^{41b,41a}, G. Tateno¹⁶², A. Tavares Delgado^{138a}, Y. Tayalati^{35f}, G.N. Taylor¹⁰⁴,
 W. Taylor^{166b}, H. Teagle⁹⁰, A.S. Tee⁸⁹, R. Teixeira De Lima¹⁵², P. Teixeira-Dias⁹³,
 H. Ten Kate³⁶, J.J. Teoh¹¹⁹, K. Terashi¹⁶², J. Terron⁹⁸, S. Terzo¹⁴, M. Testa⁵¹,
 R.J. Teuscher^{165,aa}, N. Themistokleous⁵⁰, T. Theveneaux-Pelzer¹⁹, D.W. Thomas⁹³,
 J.P. Thomas²¹, E.A. Thompson⁴⁶, P.D. Thompson²¹, E. Thomson¹³⁵, E.J. Thorpe⁹²,
 V.O. Tikhomirov^{110,ag}, Yu.A. Tikhonov^{121b,121a}, S. Timoshenko¹¹¹, P. Tipton¹⁸¹, S. Tisserant¹⁰¹,
 K. Todome^{23b,23a}, S. Todorova-Nova¹⁴¹, S. Todt⁴⁸, J. Tojo⁸⁷, S. Tokár^{28a}, K. Tokushuku⁸¹,
 E. Tolley¹²⁶, R. Tombs³², M. Tomoto^{81,116}, L. Tompkins¹⁵², P. Tornambe¹⁰², E. Torrence¹³⁰,
 H. Torres⁴⁸, E. Torró Pastor¹⁷², M. Toscani³⁰, C. Tosciri¹³³, J. Toth^{101,z}, D.R. Tovey¹⁴⁸,
 A. Traeet¹⁷, C.J. Treado¹²⁴, T. Trefzger¹⁷⁵, F. Tresoldi¹⁵⁵, A. Tricoli²⁹, I.M. Trigger^{166a},
 S. Trincaz-Duvold¹³⁴, D.A. Trischuk¹⁷³, W. Trischuk¹⁶⁵, B. Trocme⁵⁸, A. Trofymov⁶⁴,
 C. Troncon^{68a}, F. Trovato¹⁵⁵, L. Truong^{33c}, M. Trzebinski⁸⁴, A. Trzupek⁸⁴, F. Tsai⁴⁶,
 P.V. Tsiarshka^{107,ae}, A. Tsirigotis^{161,v}, V. Tsiskaridze¹⁵⁴, E.G. Tskhadadze^{158a},
 M. Tsopoulou¹⁶¹, I.I. Tsukerman¹²³, V. Tsulaia¹⁸, S. Tsuno⁸¹, D. Tsybychev¹⁵⁴, Y. Tu^{62b},
 A. Tudorache^{27b}, V. Tudorache^{27b}, A.N. Tuna³⁶, S. Turchikhin⁷⁹, D. Turgeman¹⁷⁸,
 I. Turk Cakir^{4b,t}, R.J. Turner²¹, R. Turra^{68a}, P.M. Tuts³⁹, S. Tzamarias¹⁶¹, E. Tzovara⁹⁹,
 K. Uchida¹⁶², F. Ukegawa¹⁶⁷, G. Unal³⁶, M. Unal¹¹, A. Undrus²⁹, G. Unel¹⁶⁹, F.C. Ungaro¹⁰⁴,
 K. Uno¹⁶², J. Urban^{28b}, P. Urquijo¹⁰⁴, G. Usai⁸, Z. Uysal^{12d}, V. Vacek¹⁴⁰, B. Vachon¹⁰³,
 K.O.H. Vadla¹³², T. Vafeiadis³⁶, A. Vaidya⁹⁴, C. Valderanis¹¹³, E. Valdes Santurio^{45a,45b},
 M. Valente^{166a}, S. Valentineti^{23b,23a}, A. Valero¹⁷², L. Valéry⁴⁶, R.A. Vallance²¹, A. Vallier³⁶,
 J.A. Valls Ferrer¹⁷², T.R. Van Daalen¹⁴, P. Van Gemmeren⁶, S. Van Stroud⁹⁴, I. Van Vulpen¹¹⁹,
 M. Vanadia^{73a,73b}, W. Vandelli³⁶, M. Vandenbroucke¹⁴³, E.R. Vandewall¹²⁸, D. Vannicola^{72a,72b},
 R. Vari^{72a}, E.W. Varnes⁷, C. Varni^{55b,55a}, T. Varol¹⁵⁷, D. Varouchas⁶⁴, K.E. Varvell¹⁵⁶,
 M.E. Vasile^{27b}, G.A. Vasquez¹⁷⁴, F. Vazeille³⁸, D. Vazquez Furelos¹⁴, T. Vazquez Schroeder³⁶,
 J. Veatch⁵³, V. Vecchio¹⁰⁰, M.J. Veen¹¹⁹, L.M. Veloce¹⁶⁵, F. Veloso^{138a,138c}, S. Veneziano^{72a},
 A. Ventura^{67a,67b}, A. Verbytskyi¹¹⁴, M. Verducci^{71a,71b}, C. Vergis²⁴, W. Verkerke¹¹⁹,
 A.T. Vermeulen¹¹⁹, J.C. Vermeulen¹¹⁹, C. Vernieri¹⁵², P.J. Verschuuren⁹³, M.C. Vetterli^{151,ak},
 N. Viaux Maira^{145d}, T. Vickey¹⁴⁸, O.E. Vickey Boeriu¹⁴⁸, G.H.A. Viehhauser¹³³, L. Vigani^{61b},
 M. Villa^{23b,23a}, M. Villaplana Perez¹⁷², E.M. Villhauer⁵⁰, E. Vilucchi⁵¹, M.G. Vincter³⁴,
 G.S. Virdee²¹, A. Vishwakarma⁵⁰, C. Vittori^{23b,23a}, I. Vivarelli¹⁵⁵, M. Vogel¹⁸⁰, P. Vokac¹⁴⁰,
 J. Von Ahnen⁴⁶, S.E. von Buddenbrock^{33e}, E. Von Toerne²⁴, V. Vorobel¹⁴¹, K. Vorobev¹¹¹,
 M. Vos¹⁷², J.H. Vosseveld⁹⁰, M. Vozak¹⁰⁰, N. Vranjes¹⁶, M. Vranjes Milosavljevic¹⁶, V. Vrba^{140,*},
 M. Vreeswijk¹¹⁹, N.K. Vu¹⁰¹, R. Vuillermet³⁶, I. Vukotic³⁷, S. Wada¹⁶⁷, C. Wagner¹⁰²,
 P. Wagner²⁴, W. Wagner¹⁸⁰, S. Wahdan¹⁸⁰, H. Wahlberg⁸⁸, R. Wakasa¹⁶⁷, V.M. Walbrecht¹¹⁴,
 J. Walder¹⁴², R. Walker¹¹³, S.D. Walker⁹³, W. Walkowiak¹⁵⁰, V. Wallangen^{45a,45b}, A.M. Wang⁵⁹,
 A.Z. Wang¹⁷⁹, C. Wang^{60a}, C. Wang^{60c}, H. Wang¹⁸, J. Wang^{62a}, P. Wang⁴², R.-J. Wang⁹⁹,
 R. Wang^{60a}, R. Wang¹²⁰, S.M. Wang¹⁵⁷, S. Wang^{60b}, T. Wang^{60a}, W.T. Wang^{60a}, W.X. Wang^{60a},
 Y. Wang^{60a}, Z. Wang¹⁰⁵, C. Wanotayaroj³⁶, A. Warburton¹⁰³, C.P. Ward³², R.J. Ward²¹,
 N. Warrack⁵⁷, A.T. Watson²¹, M.F. Watson²¹, G. Watts¹⁴⁷, B.M. Waugh⁹⁴, A.F. Webb¹¹,
 C. Weber²⁹, M.S. Weber²⁰, S.A. Weber³⁴, S.M. Weber^{61a}, Y. Wei¹³³, A.R. Weidberg¹³³,
 J. Weingarten⁴⁷, M. Weirich⁹⁹, C. Weiser⁵², P.S. Wells³⁶, T. Wenaus²⁹, B. Wendland⁴⁷,
 T. Wengler³⁶, S. Wenig³⁶, N. Wermes²⁴, M. Wessels^{61a}, T.D. Weston²⁰, K. Whalen¹³⁰,
 A.M. Wharton⁸⁹, A.S. White¹⁰⁵, A. White⁸, M.J. White¹, D. Whiteson¹⁶⁹, B.W. Whitmore⁸⁹,
 W. Wiedenmann¹⁷⁹, C. Wiel⁴⁸, M. Wielers¹⁴², N. Wieseotte⁹⁹, C. Wiglesworth⁴⁰,
 L.A.M. Wiik-Fuchs⁵², H.G. Wilkens³⁶, L.J. Wilkins⁹³, D.M. Williams³⁹, H.H. Williams¹³⁵,

S. Williams³², S. Willocq¹⁰², P.J. Windischhofer¹³³, I. Wingerter-Seez⁵, E. Winkels¹⁵⁵,
 F. Winklmeier¹³⁰, B.T. Winter⁵², M. Wittgen¹⁵², M. Wobisch⁹⁵, A. Wolf⁹⁹, R. Wölker¹³³,
 J. Wollrath⁵², M.W. Wolter⁸⁴, H. Wolters^{138a,138c}, V.W.S. Wong¹⁷³, A.F. Wongel⁴⁶,
 N.L. Woods¹⁴⁴, S.D. Worm⁴⁶, B.K. Wosiek⁸⁴, K.W. Woźniak⁸⁴, K. Wraight⁵⁷, S.L. Wu¹⁷⁹,
 X. Wu⁵⁴, Y. Wu^{60a}, J. Wuerzinger¹³³, T.R. Wyatt¹⁰⁰, B.M. Wynne⁵⁰, S. Xella⁴⁰, J. Xiang^{62c},
 X. Xiao¹⁰⁵, X. Xie^{60a}, I. Xiotidis¹⁵⁵, D. Xu^{15a}, H. Xu^{60a}, H. Xu^{60a}, L. Xu²⁹, R. Xu¹³⁵, T. Xu¹⁴³,
 W. Xu¹⁰⁵, Y. Xu^{15b}, Z. Xu^{60b}, Z. Xu¹⁵², B. Yabsley¹⁵⁶, S. Yacoob^{33a}, D.P. Yallup⁹⁴,
 N. Yamaguchi⁸⁷, Y. Yamaguchi¹⁶³, M. Yamatani¹⁶², H. Yamauchi¹⁶⁷, T. Yamazaki¹⁸,
 Y. Yamazaki⁸², J. Yan^{60c}, Z. Yan²⁵, H.J. Yang^{60c,60d}, H.T. Yang¹⁸, S. Yang^{60a}, T. Yang^{62c},
 X. Yang^{60a}, X. Yang^{15a}, Y. Yang¹⁶², Z. Yang^{60a}, W.-M. Yao¹⁸, Y.C. Yap⁴⁶, H. Ye^{15c}, J. Ye⁴²,
 S. Ye²⁹, I. Yeletsikh⁷⁹, M.R. Yexley⁸⁹, P. Yin³⁹, K. Yorita¹⁷⁷, K. Yoshihara⁷⁸, C.J.S. Young³⁶,
 C. Young¹⁵², R. Yuan^{60b,i}, X. Yue^{61a}, M. Zaazoua^{35f}, B. Zabinski⁸⁴, G. Zacharis¹⁰, E. Zaffaroni⁵⁴,
 J. Zahreddine¹³⁴, A.M. Zaitsev^{122,af}, T. Zakareishvili^{158b}, N. Zakharchuk³⁴, S. Zambito³⁶,
 D. Zanzi⁵², S.V. Zeißner⁴⁷, C. Zeitnitz¹⁸⁰, G. Zemaityte¹³³, J.C. Zeng¹⁷¹, O. Zenin¹²², T. Ženis^{28a},
 S. Zenz⁹², S. Zerradi^{35a}, D. Zerwas⁶⁴, M. Zgubic¹³³, B. Zhang^{15c}, D.F. Zhang^{15b}, G. Zhang^{15b},
 J. Zhang⁶, K. Zhang^{15a}, L. Zhang^{15c}, L. Zhang^{60a}, M. Zhang¹⁷¹, R. Zhang¹⁷⁹, S. Zhang¹⁰⁵,
 X. Zhang^{60c}, X. Zhang^{60b}, Y. Zhang^{15a,15d}, Z. Zhang⁶⁴, P. Zhao⁴⁹, Y. Zhao¹⁴⁴, Z. Zhao^{60a},
 A. Zhemchugov⁷⁹, Z. Zheng¹⁰⁵, D. Zhong¹⁷¹, B. Zhou¹⁰⁵, C. Zhou¹⁷⁹, H. Zhou⁷, M. Zhou¹⁵⁴,
 N. Zhou^{60c}, Y. Zhou⁷, C.G. Zhu^{60b}, C. Zhu^{15a,15d}, H.L. Zhu^{60a}, H. Zhu^{15a}, J. Zhu¹⁰⁵, Y. Zhu^{60a},
 X. Zhuang^{15a}, K. Zhukov¹¹⁰, V. Zhulanov^{121b,121a}, D. Ziemska⁶⁵, N.I. Zimine⁷⁹,
 S. Zimmermann^{52,*}, Z. Zinonos¹¹⁴, M. Ziolkowski¹⁵⁰, L. Živković¹⁶, A. Zoccolì^{23b,23a}, K. Zoch⁵³,
 T.G. Zorbas¹⁴⁸, R. Zou³⁷, L. Zwalinski³⁶

¹ Department of Physics, University of Adelaide, Adelaide, Australia

² Physics Department, SUNY Albany, Albany NY, U.S.A.

³ Department of Physics, University of Alberta, Edmonton AB, Canada

⁴ ^(a) Department of Physics, Ankara University, Ankara, ^(b) Istanbul Aydin University, Application and Research Center for Advanced Studies, Istanbul, ^(c) Division of Physics, TOBB University of Economics and Technology, Ankara, Turkey

⁵ LAPP, Université Grenoble Alpes, Université Savoie Mont Blanc, CNRS/IN2P3, Annecy, France

⁶ High Energy Physics Division, Argonne National Laboratory, Argonne IL, U.S.A.

⁷ Department of Physics, University of Arizona, Tucson AZ, U.S.A.

⁸ Department of Physics, University of Texas at Arlington, Arlington TX, U.S.A.

⁹ Physics Department, National and Kapodistrian University of Athens, Athens, Greece

¹⁰ Physics Department, National Technical University of Athens, Zografou, Greece

¹¹ Department of Physics, University of Texas at Austin, Austin TX, U.S.A.

¹² ^(a) Bahcesehir University, Faculty of Engineering and Natural Sciences, Istanbul, ^(b) Istanbul Bilgi University, Faculty of Engineering and Natural Sciences, Istanbul, ^(c) Department of Physics, Bogazici University, Istanbul, ^(d) Department of Physics Engineering, Gaziantep University, Gaziantep, Turkey

¹³ Institute of Physics, Azerbaijan Academy of Sciences, Baku, Azerbaijan

¹⁴ Institut de Física d'Altes Energies (IFAE), Barcelona Institute of Science and Technology, Barcelona, Spain

¹⁵ ^(a) Institute of High Energy Physics, Chinese Academy of Sciences, Beijing, ^(b) Physics Department, Tsinghua University, Beijing, ^(c) Department of Physics, Nanjing University, Nanjing, ^(d) University of Chinese Academy of Science (UCAS), Beijing, China

¹⁶ Institute of Physics, University of Belgrade, Belgrade, Serbia

¹⁷ Department for Physics and Technology, University of Bergen, Bergen, Norway

¹⁸ Physics Division, Lawrence Berkeley National Laboratory and University of California, Berkeley CA, U.S.A.

- ¹⁹ *Institut für Physik, Humboldt Universität zu Berlin, Berlin, Germany*
- ²⁰ *Albert Einstein Center for Fundamental Physics and Laboratory for High Energy Physics, University of Bern, Bern, Switzerland*
- ²¹ *School of Physics and Astronomy, University of Birmingham, Birmingham, U.K.*
- ²² ^(a) *Facultad de Ciencias y Centro de Investigaciones, Universidad Antonio Nariño, Bogotá,* ^(b) *Departamento de Física, Universidad Nacional de Colombia, Bogotá, Colombia, Colombia*
- ²³ ^(a) *INFN Bologna and Università di Bologna, Dipartimento di Fisica,* ^(b) *INFN Sezione di Bologna, Italy*
- ²⁴ *Physikalisches Institut, Universität Bonn, Bonn, Germany*
- ²⁵ *Department of Physics, Boston University, Boston MA, U.S.A.*
- ²⁶ *Department of Physics, Brandeis University, Waltham MA, U.S.A.*
- ²⁷ ^(a) *Transilvania University of Brasov, Brasov,* ^(b) *Horia Hulubei National Institute of Physics and Nuclear Engineering, Bucharest,* ^(c) *Department of Physics, Alexandru Ioan Cuza University of Iasi, Iasi,* ^(d) *National Institute for Research and Development of Isotopic and Molecular Technologies, Physics Department, Cluj-Napoca,* ^(e) *University Politehnica Bucharest, Bucharest,* ^(f) *West University in Timisoara, Timisoara, Romania*
- ²⁸ ^(a) *Faculty of Mathematics, Physics and Informatics, Comenius University, Bratislava,* ^(b) *Department of Subnuclear Physics, Institute of Experimental Physics of the Slovak Academy of Sciences, Kosice, Slovak Republic*
- ²⁹ *Physics Department, Brookhaven National Laboratory, Upton NY, U.S.A.*
- ³⁰ *Departamento de Física, Universidad de Buenos Aires, Buenos Aires, Argentina*
- ³¹ *California State University, CA, U.S.A.*
- ³² *Cavendish Laboratory, University of Cambridge, Cambridge, U.K.*
- ³³ ^(a) *Department of Physics, University of Cape Town, Cape Town,* ^(b) *iThemba Labs, Western Cape,* ^(c) *Department of Mechanical Engineering Science, University of Johannesburg, Johannesburg,* ^(d) *University of South Africa, Department of Physics, Pretoria,* ^(e) *School of Physics, University of the Witwatersrand, Johannesburg, South Africa*
- ³⁴ *Department of Physics, Carleton University, Ottawa ON, Canada*
- ³⁵ ^(a) *Faculté des Sciences Ain Chock, Réseau Universitaire de Physique des Hautes Energies - Université Hassan II, Casablanca,* ^(b) *Faculté des Sciences, Université Ibn-Tofail, Kénitra,* ^(c) *Faculté des Sciences Semlalia, Université Cadi Ayyad, LPHEA-Marrakech,* ^(d) *Moroccan Foundation for Advanced Science Innovation and Research (MAScIR), Rabat,* ^(e) *LPMR, Faculté des Sciences, Université Mohamed Premier, Oujda,* ^(f) *Faculté des sciences, Université Mohammed V, Rabat, Morocco*
- ³⁶ *CERN, Geneva, Switzerland*
- ³⁷ *Enrico Fermi Institute, University of Chicago, Chicago IL, U.S.A.*
- ³⁸ *LPC, Université Clermont Auvergne, CNRS/IN2P3, Clermont-Ferrand, France*
- ³⁹ *Nevis Laboratory, Columbia University, Irvington NY, U.S.A.*
- ⁴⁰ *Niels Bohr Institute, University of Copenhagen, Copenhagen, Denmark*
- ⁴¹ ^(a) *Dipartimento di Fisica, Università della Calabria, Rende,* ^(b) *INFN Gruppo Collegato di Cosenza, Laboratori Nazionali di Frascati, Italy*
- ⁴² *Physics Department, Southern Methodist University, Dallas TX, U.S.A.*
- ⁴³ *Physics Department, University of Texas at Dallas, Richardson TX, U.S.A.*
- ⁴⁴ *National Centre for Scientific Research "Demokritos", Agia Paraskevi, Greece*
- ⁴⁵ ^(a) *Department of Physics, Stockholm University,* ^(b) *Oskar Klein Centre, Stockholm, Sweden*
- ⁴⁶ *Deutsches Elektronen-Synchrotron DESY, Hamburg and Zeuthen, Germany*
- ⁴⁷ *Lehrstuhl für Experimentelle Physik IV, Technische Universität Dortmund, Dortmund, Germany*
- ⁴⁸ *Institut für Kern- und Teilchenphysik, Technische Universität Dresden, Dresden, Germany*
- ⁴⁹ *Department of Physics, Duke University, Durham NC, U.S.A.*
- ⁵⁰ *SUPA - School of Physics and Astronomy, University of Edinburgh, Edinburgh, U.K.*
- ⁵¹ *INFN e Laboratori Nazionali di Frascati, Frascati, Italy*
- ⁵² *Physikalisches Institut, Albert-Ludwigs-Universität Freiburg, Freiburg, Germany*

- 53 *II. Physikalisches Institut, Georg-August-Universität Göttingen, Göttingen, Germany*
- 54 *Département de Physique Nucléaire et Corpusculaire, Université de Genève, Genève, Switzerland*
- 55 ^(a) *Dipartimento di Fisica, Università di Genova, Genova,* ^(b) *INFN Sezione di Genova, Italy*
- 56 *II. Physikalisches Institut, Justus-Liebig-Universität Giessen, Giessen, Germany*
- 57 *SUPA - School of Physics and Astronomy, University of Glasgow, Glasgow, U.K.*
- 58 *LPSC, Université Grenoble Alpes, CNRS/IN2P3, Grenoble INP, Grenoble, France*
- 59 *Laboratory for Particle Physics and Cosmology, Harvard University, Cambridge MA, U.S.A.*
- 60 ^(a) *Department of Modern Physics and State Key Laboratory of Particle Detection and Electronics, University of Science and Technology of China, Hefei,* ^(b) *Institute of Frontier and Interdisciplinary Science and Key Laboratory of Particle Physics and Particle Irradiation (MOE), Shandong University, Qingdao,* ^(c) *School of Physics and Astronomy, Shanghai Jiao Tong University, Key Laboratory for Particle Astrophysics and Cosmology (MOE), SKLPPC, Shanghai,* ^(d) *Tsung-Dao Lee Institute, Shanghai, China*
- 61 ^(a) *Kirchhoff-Institut für Physik, Ruprecht-Karls-Universität Heidelberg, Heidelberg,*
- ^(b) *Physikalisches Institut, Ruprecht-Karls-Universität Heidelberg, Heidelberg, Germany*
- 62 ^(a) *Department of Physics, Chinese University of Hong Kong, Shatin, N.T., Hong Kong,*
- ^(b) *Department of Physics, University of Hong Kong, Hong Kong,* ^(c) *Department of Physics and Institute for Advanced Study, Hong Kong University of Science and Technology, Clear Water Bay, Kowloon, Hong Kong, China*
- 63 *Department of Physics, National Tsing Hua University, Hsinchu, Taiwan*
- 64 *IJCLab, Université Paris-Saclay, CNRS/IN2P3, 91405, Orsay, France*
- 65 *Department of Physics, Indiana University, Bloomington IN, U.S.A.*
- 66 ^(a) *INFN Gruppo Collegato di Udine, Sezione di Trieste, Udine,* ^(b) *ICTP, Trieste,* ^(c) *Dipartimento Politecnico di Ingegneria e Architettura, Università di Udine, Udine, Italy*
- 67 ^(a) *INFN Sezione di Lecce,* ^(b) *Dipartimento di Matematica e Fisica, Università del Salento, Lecce, Italy*
- 68 ^(a) *INFN Sezione di Milano,* ^(b) *Dipartimento di Fisica, Università di Milano, Milano, Italy*
- 69 ^(a) *INFN Sezione di Napoli,* ^(b) *Dipartimento di Fisica, Università di Napoli, Napoli, Italy*
- 70 ^(a) *INFN Sezione di Pavia,* ^(b) *Dipartimento di Fisica, Università di Pavia, Pavia, Italy*
- 71 ^(a) *INFN Sezione di Pisa,* ^(b) *Dipartimento di Fisica E. Fermi, Università di Pisa, Pisa, Italy*
- 72 ^(a) *INFN Sezione di Roma,* ^(b) *Dipartimento di Fisica, Sapienza Università di Roma, Roma, Italy*
- 73 ^(a) *INFN Sezione di Roma Tor Vergata,* ^(b) *Dipartimento di Fisica, Università di Roma Tor Vergata, Roma, Italy*
- 74 ^(a) *INFN Sezione di Roma Tre,* ^(b) *Dipartimento di Matematica e Fisica, Università Roma Tre, Roma, Italy*
- 75 ^(a) *INFN-TIFPA,* ^(b) *Università degli Studi di Trento, Trento, Italy*
- 76 *Institut für Astro- und Teilchenphysik, Leopold-Franzens-Universität, Innsbruck, Austria*
- 77 *University of Iowa, Iowa City IA, U.S.A.*
- 78 *Department of Physics and Astronomy, Iowa State University, Ames IA, U.S.A.*
- 79 *Joint Institute for Nuclear Research, Dubna, Russia*
- 80 ^(a) *Departamento de Engenharia Elétrica, Universidade Federal de Juiz de Fora (UFJF), Juiz de Fora,* ^(b) *Universidade Federal do Rio De Janeiro COPPE/EE/IF, Rio de Janeiro,* ^(c) *Instituto de Física, Universidade de São Paulo, São Paulo, Brazil*
- 81 *KEK, High Energy Accelerator Research Organization, Tsukuba, Japan*
- 82 *Graduate School of Science, Kobe University, Kobe, Japan*
- 83 ^(a) *AGH University of Science and Technology, Faculty of Physics and Applied Computer Science, Krakow,* ^(b) *Marian Smoluchowski Institute of Physics, Jagiellonian University, Krakow, Poland*
- 84 *Institute of Nuclear Physics Polish Academy of Sciences, Krakow, Poland*
- 85 *Faculty of Science, Kyoto University, Kyoto, Japan*
- 86 *Kyoto University of Education, Kyoto, Japan*
- 87 *Research Center for Advanced Particle Physics and Department of Physics, Kyushu University, Fukuoka, Japan*

- ⁸⁸ *Instituto de Física La Plata, Universidad Nacional de La Plata and CONICET, La Plata, Argentina*
- ⁸⁹ *Physics Department, Lancaster University, Lancaster, U.K.*
- ⁹⁰ *Oliver Lodge Laboratory, University of Liverpool, Liverpool, U.K.*
- ⁹¹ *Department of Experimental Particle Physics, Jožef Stefan Institute and Department of Physics, University of Ljubljana, Ljubljana, Slovenia*
- ⁹² *School of Physics and Astronomy, Queen Mary University of London, London, U.K.*
- ⁹³ *Department of Physics, Royal Holloway University of London, Egham, U.K.*
- ⁹⁴ *Department of Physics and Astronomy, University College London, London, U.K.*
- ⁹⁵ *Louisiana Tech University, Ruston LA, U.S.A.*
- ⁹⁶ *Fysiska institutionen, Lunds universitet, Lund, Sweden*
- ⁹⁷ *Centre de Calcul de l'Institut National de Physique Nucléaire et de Physique des Particules (IN2P3), Villeurbanne, France*
- ⁹⁸ *Departamento de Física Teórica C-15 and CIAFF, Universidad Autónoma de Madrid, Madrid, Spain*
- ⁹⁹ *Institut für Physik, Universität Mainz, Mainz, Germany*
- ¹⁰⁰ *School of Physics and Astronomy, University of Manchester, Manchester, U.K.*
- ¹⁰¹ *CPPM, Aix-Marseille Université, CNRS/IN2P3, Marseille, France*
- ¹⁰² *Department of Physics, University of Massachusetts, Amherst MA, U.S.A.*
- ¹⁰³ *Department of Physics, McGill University, Montreal QC, Canada*
- ¹⁰⁴ *School of Physics, University of Melbourne, Victoria, Australia*
- ¹⁰⁵ *Department of Physics, University of Michigan, Ann Arbor MI, U.S.A.*
- ¹⁰⁶ *Department of Physics and Astronomy, Michigan State University, East Lansing MI, U.S.A.*
- ¹⁰⁷ *B.I. Stepanov Institute of Physics, National Academy of Sciences of Belarus, Minsk, Belarus*
- ¹⁰⁸ *Research Institute for Nuclear Problems of Byelorussian State University, Minsk, Belarus*
- ¹⁰⁹ *Group of Particle Physics, University of Montreal, Montreal QC, Canada*
- ¹¹⁰ *P.N. Lebedev Physical Institute of the Russian Academy of Sciences, Moscow, Russia*
- ¹¹¹ *National Research Nuclear University MEPhI, Moscow, Russia*
- ¹¹² *D.V. Skobel'syn Institute of Nuclear Physics, M.V. Lomonosov Moscow State University, Moscow, Russia*
- ¹¹³ *Fakultät für Physik, Ludwig-Maximilians-Universität München, München, Germany*
- ¹¹⁴ *Max-Planck-Institut für Physik (Werner-Heisenberg-Institut), München, Germany*
- ¹¹⁵ *Nagasaki Institute of Applied Science, Nagasaki, Japan*
- ¹¹⁶ *Graduate School of Science and Kobayashi-Maskawa Institute, Nagoya University, Nagoya, Japan*
- ¹¹⁷ *Department of Physics and Astronomy, University of New Mexico, Albuquerque NM, U.S.A.*
- ¹¹⁸ *Institute for Mathematics, Astrophysics and Particle Physics, Radboud University/Nikhef, Nijmegen, Netherlands*
- ¹¹⁹ *Nikhef National Institute for Subatomic Physics and University of Amsterdam, Amsterdam, Netherlands*
- ¹²⁰ *Department of Physics, Northern Illinois University, DeKalb IL, U.S.A.*
- ¹²¹ ^(a) *Budker Institute of Nuclear Physics and NSU, SB RAS, Novosibirsk,* ^(b) *Novosibirsk State University Novosibirsk, Russia*
- ¹²² *Institute for High Energy Physics of the National Research Centre Kurchatov Institute, Protvino, Russia*
- ¹²³ *Institute for Theoretical and Experimental Physics named by A.I. Alikhanov of National Research Centre "Kurchatov Institute", Moscow, Russia*
- ¹²⁴ *Department of Physics, New York University, New York NY, U.S.A.*
- ¹²⁵ *Ochanomizu University, Otsuka, Bunkyo-ku, Tokyo, Japan*
- ¹²⁶ *Ohio State University, Columbus OH, U.S.A.*
- ¹²⁷ *Homer L. Dodge Department of Physics and Astronomy, University of Oklahoma, Norman OK, U.S.A.*
- ¹²⁸ *Department of Physics, Oklahoma State University, Stillwater OK, U.S.A.*
- ¹²⁹ *Palacký University, RCPTM, Joint Laboratory of Optics, Olomouc, Czech Republic*

- 130 *Institute for Fundamental Science, University of Oregon, Eugene, OR, U.S.A.*
- 131 *Graduate School of Science, Osaka University, Osaka, Japan*
- 132 *Department of Physics, University of Oslo, Oslo, Norway*
- 133 *Department of Physics, Oxford University, Oxford, U.K.*
- 134 *LPNHE, Sorbonne Université, Université de Paris, CNRS/IN2P3, Paris, France*
- 135 *Department of Physics, University of Pennsylvania, Philadelphia PA, U.S.A.*
- 136 *Konstantinov Nuclear Physics Institute of National Research Centre "Kurchatov Institute", PNPI, St. Petersburg, Russia*
- 137 *Department of Physics and Astronomy, University of Pittsburgh, Pittsburgh PA, U.S.A.*
- 138 (a) *Laboratório de Instrumentação e Física Experimental de Partículas - LIP, Lisboa,*
 (b) *Departamento de Física, Faculdade de Ciências, Universidade de Lisboa, Lisboa,*
 (c) *Departamento de Física, Universidade de Coimbra, Coimbra,* (d) *Centro de Física Nuclear da Universidade de Lisboa, Lisboa,* (e) *Departamento de Física, Universidade do Minho, Braga,*
 (f) *Departamento de Física Teórica y del Cosmos, Universidad de Granada, Granada (Spain),*
 (g) *Dep Física and CEFITEC of Faculdade de Ciências e Tecnologia, Universidade Nova de Lisboa, Caparica,* (h) *Instituto Superior Técnico, Universidade de Lisboa, Lisboa, Portugal*
- 139 *Institute of Physics of the Czech Academy of Sciences, Prague, Czech Republic*
- 140 *Czech Technical University in Prague, Prague, Czech Republic*
- 141 *Charles University, Faculty of Mathematics and Physics, Prague, Czech Republic*
- 142 *Particle Physics Department, Rutherford Appleton Laboratory, Didcot, U.K.*
- 143 *IRFU, CEA, Université Paris-Saclay, Gif-sur-Yvette, France*
- 144 *Santa Cruz Institute for Particle Physics, University of California Santa Cruz, Santa Cruz CA, U.S.A.*
- 145 (a) *Departamento de Física, Pontificia Universidad Católica de Chile, Santiago,* (b) *Universidad Andres Bello, Department of Physics, Santiago,* (c) *Instituto de Alta Investigación, Universidad de Tarapacá,* (d) *Departamento de Física, Universidad Técnica Federico Santa María, Valparaíso, Chile*
- 146 *Universidade Federal de São João del Rei (UFSJ), São João del Rei, Brazil*
- 147 *Department of Physics, University of Washington, Seattle WA, U.S.A.*
- 148 *Department of Physics and Astronomy, University of Sheffield, Sheffield, U.K.*
- 149 *Department of Physics, Shinshu University, Nagano, Japan*
- 150 *Department Physik, Universität Siegen, Siegen, Germany*
- 151 *Department of Physics, Simon Fraser University, Burnaby BC, Canada*
- 152 *SLAC National Accelerator Laboratory, Stanford CA, U.S.A.*
- 153 *Physics Department, Royal Institute of Technology, Stockholm, Sweden*
- 154 *Departments of Physics and Astronomy, Stony Brook University, Stony Brook NY, U.S.A.*
- 155 *Department of Physics and Astronomy, University of Sussex, Brighton, U.K.*
- 156 *School of Physics, University of Sydney, Sydney, Australia*
- 157 *Institute of Physics, Academia Sinica, Taipei, Taiwan*
- 158 (a) *E. Andronikashvili Institute of Physics, Iv. Javakishvili Tbilisi State University, Tbilisi,* (b) *High Energy Physics Institute, Tbilisi State University, Tbilisi, Georgia*
- 159 *Department of Physics, Technion, Israel Institute of Technology, Haifa, Israel*
- 160 *Raymond and Beverly Sackler School of Physics and Astronomy, Tel Aviv University, Tel Aviv, Israel*
- 161 *Department of Physics, Aristotle University of Thessaloniki, Thessaloniki, Greece*
- 162 *International Center for Elementary Particle Physics and Department of Physics, University of Tokyo, Tokyo, Japan*
- 163 *Department of Physics, Tokyo Institute of Technology, Tokyo, Japan*
- 164 *Tomsk State University, Tomsk, Russia*
- 165 *Department of Physics, University of Toronto, Toronto ON, Canada*
- 166 (a) *TRIUMF, Vancouver BC,* (b) *Department of Physics and Astronomy, York University, Toronto ON, Canada*

- ¹⁶⁷ *Division of Physics and Tomonaga Center for the History of the Universe, Faculty of Pure and Applied Sciences, University of Tsukuba, Tsukuba, Japan*
- ¹⁶⁸ *Department of Physics and Astronomy, Tufts University, Medford MA, U.S.A.*
- ¹⁶⁹ *Department of Physics and Astronomy, University of California Irvine, Irvine CA, U.S.A.*
- ¹⁷⁰ *Department of Physics and Astronomy, University of Uppsala, Uppsala, Sweden*
- ¹⁷¹ *Department of Physics, University of Illinois, Urbana IL, U.S.A.*
- ¹⁷² *Instituto de Física Corpuscular (IFIC), Centro Mixto Universidad de Valencia - CSIC, Valencia, Spain*
- ¹⁷³ *Department of Physics, University of British Columbia, Vancouver BC, Canada*
- ¹⁷⁴ *Department of Physics and Astronomy, University of Victoria, Victoria BC, Canada*
- ¹⁷⁵ *Fakultät für Physik und Astronomie, Julius-Maximilians-Universität Würzburg, Würzburg, Germany*
- ¹⁷⁶ *Department of Physics, University of Warwick, Coventry, U.K.*
- ¹⁷⁷ *Waseda University, Tokyo, Japan*
- ¹⁷⁸ *Department of Particle Physics and Astrophysics, Weizmann Institute of Science, Rehovot, Israel*
- ¹⁷⁹ *Department of Physics, University of Wisconsin, Madison WI, U.S.A.*
- ¹⁸⁰ *Fakultät für Mathematik und Naturwissenschaften, Fachgruppe Physik, Bergische Universität Wuppertal, Wuppertal, Germany*
- ¹⁸¹ *Department of Physics, Yale University, New Haven CT, U.S.A.*
- ^a *Also at Borough of Manhattan Community College, City University of New York, New York NY, U.S.A.*
- ^b *Also at Center for High Energy Physics, Peking University, China*
- ^c *Also at Centro Studi e Ricerche Enrico Fermi, Italy*
- ^d *Also at CERN, Geneva, Switzerland*
- ^e *Also at CPPM, Aix-Marseille Université, CNRS/IN2P3, Marseille, France*
- ^f *Also at Département de Physique Nucléaire et Corpusculaire, Université de Genève, Genève, Switzerland*
- ^g *Also at Departament de Física de la Universitat Autònoma de Barcelona, Barcelona, Spain*
- ^h *Also at Department of Financial and Management Engineering, University of the Aegean, Chios, Greece*
- ⁱ *Also at Department of Physics and Astronomy, Michigan State University, East Lansing MI, U.S.A.*
- ^j *Also at Department of Physics and Astronomy, University of Louisville, Louisville, KY, U.S.A.*
- ^k *Also at Department of Physics, Ben Gurion University of the Negev, Beer Sheva, Israel*
- ^l *Also at Department of Physics, California State University, East Bay, U.S.A.*
- ^m *Also at Department of Physics, California State University, Fresno, U.S.A.*
- ⁿ *Also at Department of Physics, California State University, Sacramento, U.S.A.*
- ^o *Also at Department of Physics, King's College London, London, U.K.*
- ^p *Also at Department of Physics, St. Petersburg State Polytechnical University, St. Petersburg, Russia*
- ^q *Also at Department of Physics, University of Fribourg, Fribourg, Switzerland*
- ^r *Also at Dipartimento di Matematica, Informatica e Fisica, Università di Udine, Udine, Italy*
- ^s *Also at Faculty of Physics, M.V. Lomonosov Moscow State University, Moscow, Russia*
- ^t *Also at Giresun University, Faculty of Engineering, Giresun, Turkey*
- ^u *Also at Graduate School of Science, Osaka University, Osaka, Japan*
- ^v *Also at Hellenic Open University, Patras, Greece*
- ^w *Also at Institutio Catalana de Recerca i Estudis Avancats, ICREA, Barcelona, Spain*
- ^x *Also at Institut für Experimentalphysik, Universität Hamburg, Hamburg, Germany*
- ^y *Also at Institute for Nuclear Research and Nuclear Energy (INRNE) of the Bulgarian Academy of Sciences, Sofia, Bulgaria*

- ^z Also at Institute for Particle and Nuclear Physics, Wigner Research Centre for Physics, Budapest, Hungary
- ^{aa} Also at Institute of Particle Physics (IPP), Canada
- ^{ab} Also at Institute of Physics, Azerbaijan Academy of Sciences, Baku, Azerbaijan
- ^{ac} Also at Instituto de Fisica Teorica, IFT-UAM/CSIC, Madrid, Spain
- ^{ad} Also at Istanbul University, Dept. of Physics, Istanbul, Turkey
- ^{ae} Also at Joint Institute for Nuclear Research, Dubna, Russia
- ^{af} Also at Moscow Institute of Physics and Technology State University, Dolgoprudny, Russia
- ^{ag} Also at National Research Nuclear University MEPhI, Moscow, Russia
- ^{ah} Also at Physics Department, An-Najah National University, Nablus, Palestine
- ^{ai} Also at Physikalisches Institut, Albert-Ludwigs-Universität Freiburg, Freiburg, Germany
- ^{aj} Also at The City College of New York, New York NY, U.S.A.
- ^{ak} Also at TRIUMF, Vancouver BC, Canada
- ^{al} Also at Università di Napoli Parthenope, Napoli, Italy
- ^{am} Also at University of Chinese Academy of Sciences (UCAS), Beijing, China
- * Deceased